ESAIM: M2AN 59 (2025) 1271–1299
https://doi.org/10.1051/m2an/2025026

ESAIM: Mathematical Modelling and Numerical Analysis
www.esaim-m2an.org

LIMIT CONSISTENCY OF LATTICE BOLTZMANN EQUATIONS

Stephan Simonis[1,*] and Mathias J. Krause[2]

Abstract. We establish the notion of limit consistency as a modular part in proving the consistency of lattice Boltzmann equations (LBEs) with respect to a given partial differential equation (PDE) system. The incompressible Navier–Stokes equations (NSE) are used as a paragon. Based upon the hydrodynamic limit of the Bhatnagar–Gross–Krook (BGK) Boltzmann equation towards the NSE, we provide a successive discretization by nesting conventional Taylor expansions and finite differences. We track the discretization state of the domain for the particle distribution functions and measure truncation errors at all levels within the derivation procedure. By parameterizing equations and proving the limit consistency of the respective families of equations, we retain the path toward the targeted PDE at each step of discretization, that is, for the discrete velocity BGK Boltzmann equations and the space-time discretized LBEs. As a direct result, we unfold the discretization technique of lattice Boltzmann methods as chaining finite differences and provide a generic top-down derivation of the numerical scheme that upholds the continuous limit.

Mathematics Subject Classification. 65M12, 35Q20, 35Q30, 76D05.

Received February 15, 2024. Accepted March 31, 2025.

1. Introduction

Due to the interlacing of discretization and relaxation, the lattice Boltzmann method (LBM) presents distinct advantages in terms of parallelizability [31, 61]. Primarily out of this reason, meanwhile the LBM has become an established alternative to conventional approximation tools for the incompressible Navier–Stokes equations (NSE) [36] where optimized scalability to high performance computers is crucial. As such, LBMs have been used with various extensions for applicative scenarios [14, 22, 32, 34, 42, 51], such as transient and statistical computer simulations of turbulent fluid flow with the help of assistive numerical diffusion [52, 54] or large eddy simulation in space [57] and in time [55]. Nonetheless, the LBM's relaxation principle does come at the price of inducing a bottom-up method, which stands in contrast to conventional top-down discretization techniques such as finite difference methods. This intrinsic feature complicates the rigorous numerical analysis of LBMs. In addition, nonpredictable stability and thus convergence limitations for multi-relaxation-time LBMs have been indicated by exploratory computing [54] with the help of the highly parallel C++ data structure OpenLB [32]. Although several contributions towards the rigorous analysis of LBMs exist (see *e.g.* [3,15–17,23,26–28,35,59] and

Keywords and phrases. Lattice Boltzmann methods, Consistency, Convergence, Partial differential equations, Navier–Stokes equations.

[1] Institute for Applied and Numerical Mathematics, Karlsruhe Institute of Technology, Karlsruhe, Germany.

[2] Lattice Boltzmann Research Group, Karlsruhe Institute of Technology, Karlsruhe, Germany.

[*] Corresponding author: stephan.simonis@kit.edu

recently [41,60]), limitations to specific target equations or LBM formulations persist, and thus, to the knowledge of the authors, no generic theory for the top-down derivation of convergent LBMs has been established. As a first step towards an analytical toolbox which is both mathematically tractable and modular, recent works [53, 56] shift the perspective on the LBM from being exclusively suited for computational fluid dynamics towards a standalone numerical method for approximating partial differential equations (PDEs) in general. Therein, the authors propose an inverse path from the target PDE towards top-down constructed moment systems with generalized Maxwellians, which partly form the basis of many LBMs. Here, we continue this path by top-down discretization under the condition of limit preservation.

To that end, the present work establishes the abstract concept of limit consistency for the purpose of proving that the LBM-discretization retains an *a priori* given continuous limit. In particular, we recall and elaborate on the initial idea of Krause [31], where the classical consistency notion is modulated to analyze truncation errors with respect to families of equations. Based upon the proven diffusive limit [48] of the parametrized Bhatnagar–Gross–Krook Boltzmann equation (BGKBE) towards the NSE, we provide a successive discretization by nesting conventional Taylor expansions and finite differences. We measure truncation errors at all levels within the derivation procedure by keeping track of the discretization state of the domain for the particle distribution functions. Parametrizing the equations and proving the limit consistency of the respective families, we maintain the path towards the targeted PDE at each discretization step, *i.e.* for the discrete velocity BGKBE and the space-time discretized lattice Boltzmann equation (LBE). As a direct result, we unfold the discretization technique of LBMs as chaining finite differences and provide a generic top-down derivation of the numerical scheme. Validating our approach, the finite difference interpretation of the LBM matches the previous [25] and current rigorous observations [6,7,33] in the literature. In particular, the notion of limit consistency has been successfully applied to derive consistent and convergent LBMs for advection–diffusion equations and homogenized NSE [49, 50].

This paper is structured as follows. In Section 2, we introduce the continuous equations on mesoscopic and macroscopic levels, and recall the formality of the passage from one to the other. In Section 3, the notion of limit consistency is defined. In addition, we discuss the technical relevance of our approach with respect to established procedures and nuance distinct levels of rigor in the resulting convergence proofs. Consequently, we discretize the mesoscopic equations and prove that the diffusive limit is consistently upheld at each level of discretization. Section 4 summarizes and assesses the presented results and suggests future studies. The specifically used notation and relevant previous results are recalled in the Appendices A and B.

2. Continuous mathematical models

2.1. Targeted partial differential equation system

We aim to approximate the d-dimensional incompressible NSE as an initial value problem (IVP)

$$\begin{cases} \boldsymbol{\nabla}_{\boldsymbol{x}} \cdot \boldsymbol{u} = 0 & \text{in } I \times \Omega, \\ \partial_t \boldsymbol{u} + \frac{1}{\rho} \boldsymbol{\nabla}_{\boldsymbol{x}} p + \boldsymbol{\nabla}_{\boldsymbol{x}} \cdot (\boldsymbol{u} \otimes \boldsymbol{u}) - \nu \boldsymbol{\Delta}_{\boldsymbol{x}} \boldsymbol{u} = \boldsymbol{F} & \text{in } I \times \Omega, \\ \boldsymbol{u}(0, \cdot) = \boldsymbol{u}_0 & \text{in } \Omega, \end{cases} \tag{1}$$

where the spatial domain $\Omega \subseteq \mathbb{R}^d$ is periodically embedded in reals, $I \subseteq \mathbb{R}_{\geq 0}$ denotes the time interval, and $(t, \boldsymbol{x}) \in I \times \Omega$. In addition, $\boldsymbol{u} \colon I \times \Omega \to \mathbb{R}^3$ is the velocity field with a smooth initial value $\boldsymbol{u}_0$, $p \colon I \times \Omega \to \mathbb{R}$ is the scalar pressure, $\nu > 0$ prescribes a given viscosity, $\rho \colon I \times \Omega \to \mathbb{R}$ is an assumingly constant density, and $\boldsymbol{F} \colon I \times \Omega \to \mathbb{R}^d$ denotes a given force field. Unless stated otherwise, $\boldsymbol{\nabla}_{\boldsymbol{x}}$ is the gradient operator and $\boldsymbol{\Delta}_{\boldsymbol{x}}$ the Laplace operator, respectively, in space, and partial derivatives with respect to $\cdot$ are abbreviated as $\partial_\cdot := \partial/(\partial \cdot)$.

2.2. Kinetic equation system

To render this work self-standing, we first recall the results of Krause [31] and Saint-Raymond [48] at the continuous level and proceed in Section 3 with the successive discretization down to the LBE. At all discretization levels, we assure that the continuous limiting system (1) is maintained up to the desired order of magnitude in the parameter $h > 0$ associated with the discretization.

Let the domain $\Omega \subseteq \mathbb{R}^d$, with dimension $d = 3$ unless stated otherwise, frame a large number of particles interacting through the compound of a rarefied gas. Equalizing the mass $m \in \mathbb{R}_{>0}$, the particles are interpreted as molecules.

Definition 1. The state of a one-particle system is assumed to depend on position $\boldsymbol{x} \in \Omega$ and velocity $\boldsymbol{v} \in \Xi$ at time $t \in I = [t_0, t_1] \subseteq \mathbb{R}$ with $t_1 > t_0 > 0$, where $\Omega \subseteq \mathbb{R}^d$ denotes the positional space, $\Xi = \mathbb{R}^d$ is the velocity space, $\mathfrak{P} := \Omega \times \Xi$ is the phase space, and the crossing $\mathfrak{R} := I \times \Omega \times \Xi$ defines the time-phase tuple. The probability density function

$$f \colon \mathfrak{R} \to \mathbb{R}_{>0}, \big(t, \boldsymbol{x}, \boldsymbol{v}\big) \mapsto f\big(t, \boldsymbol{x}, \boldsymbol{v}\big) \tag{2}$$

tracks the dynamics of the particle distribution and hence defines the state of the system. The thus evoked evolution of probability density is reign by the Boltzmann equation (BE)

$$\left(\partial_t + \boldsymbol{v} \cdot \boldsymbol{\nabla}_{\boldsymbol{x}} + \frac{\boldsymbol{F}}{m} \cdot \boldsymbol{\nabla}_{\boldsymbol{v}}\right) f = J\big(f, f\big), \tag{3}$$

where $f(0, \cdot, \cdot) = f_0$ supplements a suitable initial condition. The operator

$$J\big(f, f\big) = \int_{\mathbb{R}^3} \int_{S^2} \big|\boldsymbol{v} - \boldsymbol{w}\big| \big[f\big(t, \boldsymbol{x}, \boldsymbol{v}'\big) f\big(t, \boldsymbol{x}, \boldsymbol{w}'\big) - f\big(t, \boldsymbol{x}, \boldsymbol{v}\big) f\big(t, \boldsymbol{x}, \boldsymbol{w}\big)\big] \,\mathrm{d}\boldsymbol{N} \,\mathrm{d}\boldsymbol{w} \tag{4}$$

models the collision, where $\mathrm{d}\boldsymbol{N}$ is the normalized surface integral with the unit vector $\boldsymbol{N} \in S^2$ and $(\boldsymbol{v}', \boldsymbol{w}')^{\mathrm{T}} = T_{\boldsymbol{N}} (\boldsymbol{v}, \boldsymbol{w})^{\mathrm{T}}$ results from the transformation $T_{\boldsymbol{N}}$ that models hard sphere collision [1].

The following quantities are moments of f created through integration over velocity.

Definition 2. Let f be given in the sense of (2). Then we define the moments

$$n_f \colon \begin{cases} I \times \Omega \to \mathbb{R}_{>0}, \\ \big(t, \boldsymbol{x}\big) \mapsto n_f\big(t, \boldsymbol{x}\big) := \displaystyle\int_{\mathbb{R}^d} f\big(t, \boldsymbol{x}, v\big) \,\mathrm{d}\boldsymbol{v}, \end{cases} \tag{5}$$

$$\rho_f \colon \begin{cases} I \times \Omega \to \mathbb{R}_{>0}, \\ \big(t, \boldsymbol{x}\big) \mapsto \rho_f\big(t, \boldsymbol{x}\big) := m n_f\big(t, \boldsymbol{x}\big), \end{cases} \tag{6}$$

$$\boldsymbol{u}_f \colon \begin{cases} I \times \Omega \to \mathbb{R}^d, \\ \big(t, \boldsymbol{x}\big) \mapsto u_f\big(t, \boldsymbol{x}\big) := \frac{1}{n_f(t, \boldsymbol{x})} \displaystyle\int_{\mathbb{R}^d} \boldsymbol{v} f\big(t, \boldsymbol{x}, \boldsymbol{v}\big) \,\mathrm{d}\boldsymbol{v}, \end{cases} \tag{7}$$

$$\mathbf{P}_f \colon \begin{cases} I \times \Omega \to \mathbb{R}^{d \times d}, \\ \big(t, \boldsymbol{x}\big) \mapsto \mathbf{P}_f\big(t, \boldsymbol{x}\big) := m \displaystyle\int_{\mathbb{R}^d} \big[\boldsymbol{v} - \boldsymbol{u}_f(t, \boldsymbol{x})\big] \otimes \big[\boldsymbol{v} - \boldsymbol{u}_f(t, \boldsymbol{x})\big] f\big(t, \boldsymbol{x}, \boldsymbol{v}\big) \,\mathrm{d}\boldsymbol{v}, \end{cases} \tag{8}$$

$$p_f \colon \begin{cases} I \times \Omega \to \mathbb{R}_{>0}, \\ \big(t, \boldsymbol{x}\big) \mapsto p_f\big(t, \boldsymbol{x}\big) := \frac{1}{d} \displaystyle\sum_{i=1}^{d} \big(\mathbf{P}_f\big)_{i,i}\big(t, \boldsymbol{x}\big), \end{cases} \tag{9}$$

respectively as particle density, mass, velocity, stress tensor, and pressure. Here and in the following, the moments of f are indexed correspondingly to $\cdot_f$.

Notably, the absolute temperature T is determined implicitly by an ideal gas assumption

$$p_f = n_f RT, \tag{10}$$

where $R > 0$ is the universal gas constant. In a dedicated order of magnitude on characteristic scales, the above moments approximate the macroscopic quantities conserved by the incompressible NSE [19]. Equilibrium states f^{eq} such that

$$J\big(f^{\mathrm{eq}}, f^{\mathrm{eq}}\big) = 0 \quad \text{in } I \times \Omega, \tag{11}$$

exist [19]. Via the gas constant $R = k_{\mathrm{B}}/m \in \mathbb{R}_{>0}$ (where k_{B} is the Boltzmann constant, and m is the particle mass), and $T \in \mathbb{R}_{>0}$, n_f and u_f, the equilibrium state is found to be of Maxwellian form

$$f^{\mathrm{eq}}\big(t, \boldsymbol{x}, \boldsymbol{v}\big) \colon \mathfrak{R} \to \mathbb{R}, \big(t, \boldsymbol{x}, \boldsymbol{v}\big) \mapsto \frac{n_f\big(t, \boldsymbol{x}\big)}{\big(2\pi RT\big)^{\frac{d}{2}}} \exp\left(- \frac{\big(\boldsymbol{v} - \boldsymbol{u}_f(t, \boldsymbol{x})\big)^2}{2RT} \right). \tag{12}$$

Remark 1. We identify f^{eq}/n_f as d-dimensional normal distribution for $\boldsymbol{v} \in \mathbb{R}^d$ with expectation $\boldsymbol{u}_f$ and covariance $RT\mathbf{I}_d$. In this regard, the arguments of f^{eq} regularly appear in terms of moments $f^{\mathrm{eq}}(n_f, \boldsymbol{u}_f, T)$ (*e.g.* [23, 28, 31, 35]).

From f^{eq}/n_f being a density function, we find

$$\rho_{f^{\mathrm{eq}}} \overset{(6)}{=} m \int\limits_{\mathbb{R}^d} f^{\mathrm{eq}}\big(t, \boldsymbol{x}, \boldsymbol{v}\big) \,\mathrm{d}\boldsymbol{v} \; = m n_f = \rho_f. \tag{13}$$

Thus

$$\boldsymbol{u}_{f^{\mathrm{eq}}} \overset{(7)}{=} \frac{1}{n_{f^{\mathrm{eq}}}} \int\limits_{\mathbb{R}^d} \boldsymbol{v} f^{\mathrm{eq}}\big(t, \boldsymbol{x}, \boldsymbol{v}\big) \,\mathrm{d}\boldsymbol{v} \; = \boldsymbol{u}_f. \tag{14}$$

The covariance matrix of f^{eq}/n_f for a perfect gas (10), verifies the conservation of pressure

$$p_{f^{\mathrm{eq}}} \overset{(9)}{=} \frac{1}{d} m \int\limits_{\mathbb{R}^d} \big(\boldsymbol{v} - \boldsymbol{u}_{f^{\mathrm{eq}}}\big)^2 f^{\mathrm{eq}}\big(t, \boldsymbol{x}, \boldsymbol{v}\big) \,\mathrm{d}\boldsymbol{v} = \frac{1}{d} m \int\limits_{\mathbb{R}^d} \big(\boldsymbol{v} - \boldsymbol{u}_f\big)^2 f^{\mathrm{eq}}\big(t, \boldsymbol{x}, \boldsymbol{v}\big) \,\mathrm{d}\boldsymbol{v} = \frac{1}{d} m n_f \sum_{i=1}^{d} RT = p_f. \tag{15}$$

Definition 3. According to Bhatnagar, Gross, and Krook (BGK) [8] we can simplify the collision operator J in (3) to

$$Q\big(f\big) \coloneqq -\frac{1}{\tau}\big(f - M_f^{\mathrm{eq}}\big) \quad \text{in } \mathfrak{R}, \tag{16}$$

where τ denotes the relaxation time between collisions, and $M_f^{\mathrm{eq}} \coloneqq f^{\mathrm{eq}}\big(t, \boldsymbol{x}, \boldsymbol{v}\big)$ is a formal particular Maxwellian determined by the zeroth and first order moments of f, n_f, and $\boldsymbol{u}_f$, respectively.

Remark 2. The conservation of both ρ_f and $\boldsymbol{u}_f$, respectively (13) and (14), is upheld, since $\ln(M_f^{\mathrm{eq}})$ is a collision invariant of Q (cf. [31], Theorem 1.5).

Definition 4. With Q from (16) implanted in (3), the BGKBE reads

$$\underbrace{\left(\partial_t + \boldsymbol{v} \cdot \boldsymbol{\nabla}_{\boldsymbol{x}} + \frac{\boldsymbol{F}}{m} \cdot \boldsymbol{\nabla}_{\boldsymbol{v}}\right)}_{=: \, \frac{\mathrm{D}}{\mathrm{D}t}} f = Q(f) \quad \text{in } \mathfrak{R}, \tag{17}$$

where $\mathrm{D}/(\mathrm{D}t)$ is referred to as the material derivative, and $f(0, \cdot, \cdot) = f_0$ sets a suitable initial condition.

Here and below, the variable f is renamed to obey (17) instead of (3).

Remark 3. The global existence of solutions to the BGKBE (17) has been rigorously proven in [45]. Weighted L^{∞} bounds and uniqueness have later been established in bounded domains [46] and in $\mathbb{R}^d$ [43].

Remark 4. Interestingly, the original BGK equation proposed in [8] is formulated with an additional prefactor n_f on the right-hand side of (17) that leads to a quadratic nonlinearity in the collision operator.

2.3. Diffusive limit

We connect the BGKBE (17) to the NSE (1) via diffusive limiting. To this end, a formal verification of the continuum balance equations (1) for the moments ρ_f and $\boldsymbol{u}_f$ in Definition 2 is conducted. Parts of the following derivation are taken from [31]. As suggested in [49], we stress that neither the derivation nor the references follow the aim of completeness, but rather are meant to illustrate the scale bridging from the BGKBE toward the incompressible NSE only. The limiting is done in three steps. Here, to derive the NSE, we take zeroth- and first-order moments of the BGKBE (Step 1) which yields an equation that is similar to the NSE up to the pressure tensor. The latter is then defined by using the expression M_f^{eq} in an ansatz that is related to Maxwell iteration (Step 2). In Step 3, based on the pressure tensor obtained, the NSE momentum equation is recovered up to second order in ϵ. A specific definition of the $\mathcal{O}$-notation is provided in Appendix A.1.

2.3.1. Step 1: Mass conservation and momentum balance

Let $f^{\star}$ be a solution to the BGKBE (17). Multiplying $m \times$ (17) and integrating over $\Xi = \mathbb{R}^d$ yields

$$\partial_t \rho_{f^\star} + \boldsymbol{\nabla}_{\boldsymbol{x}} \cdot \left(\rho_{f^\star} \boldsymbol{u}_{f^\star}\right) + \underbrace{\int_{\mathbb{R}^d} \boldsymbol{F} \cdot \boldsymbol{\nabla}_{\boldsymbol{v}} f^\star \, \mathrm{d}\boldsymbol{v}}_{=0} = -\frac{1}{\tau} \underbrace{\left(\rho_{f^\star} - \rho_{M^{\mathrm{eq}}_{f^\star}}\right)}_{\overset{(13)}{=}0} \tag{18}$$

$$\iff \partial_t \rho_{f^\star} + \boldsymbol{\nabla}_{\boldsymbol{x}} \cdot \left(\rho_{f^\star} \boldsymbol{u}_{f^\star}\right) = 0 \quad \text{in } I \times \Omega, \tag{19}$$

where the force term nulls out (cf. [31], Corollary 5.2, with $g = 1$ and $a = F$ in the respective notation). Dividing by the constant $\rho_{f^\star}$, the conservation of mass in the NSE is verified. To balance momentum, we integrate $m\boldsymbol{v} \times$ (17) over $\Xi = \mathbb{R}^d$ and obtain that

$$\partial_t \left(\rho_{f^\star} \boldsymbol{u}_{f^\star}\right) + \boldsymbol{\nabla}_{\boldsymbol{x}} \cdot \mathbf{P}_{f^\star} + \left(\rho_{f^\star} \boldsymbol{u}_{f^\star} \cdot \boldsymbol{\nabla}_{\boldsymbol{x}}\right) \boldsymbol{u}_{f^\star} + \boldsymbol{F} = 0 \quad \text{in } I \times \Omega. \tag{20}$$

The derivation of (20) closely follows a standard procedure documented for example in Section 1.3.1 in [31]. Finally, via (20)/$\rho_{f^\star}$ a balance law of momentum in conservative form is recovered. Thus, when suitably defining and simplifying $\mathbf{P}_{f^\star}$ according to the assumption of incompressible Newtonian flow, the incompressible NSE appears as the diffusive limiting system.

2.3.2. Step 2: Incompressible limit

The incompressible limit regime of the BGKBE (17) is obtained via aligning parameters to the diffusion terms (see *e.g.* [31]). Let l_{f} be the mean free path, $\bar{c}$ the mean absolute thermal velocity, and $\nu > 0$ a kinematic viscosity. Assuming that a characteristic length L and a characteristic velocity U are given, we define the Knudsen number, the Mach number, and the Reynolds number, respectively

$$Kn := \frac{l_{\mathrm{f}}}{L}, \tag{21}$$

$$Ma := \frac{U}{c_{\mathrm{s}}}, \tag{22}$$

$$Re := \frac{UL}{\nu}\cdot \tag{23}$$

These non-dimensional numbers relate as

$$Re = \frac{l_{\mathrm{f}} c_{\mathrm{s}}}{\nu} \frac{Ma}{Kn} = \sqrt{\frac{24}{\pi}} \frac{Ma}{Kn}, \tag{24}$$

via defining $\nu \coloneqq \pi \bar{c} l_{\mathrm{f}}/8$ and the isothermal speed of sound $c_{\mathrm{s}} \coloneqq \sqrt{3RT}$ (see also [48] and references therein).

Definition 5. To link the mesoscopic distributions with the macroscopic continuum we inversely substitute c_{s} with an artificial parameter $\epsilon \in \mathbb{R}_{>0}$ through

$$c_{\mathrm{s}} = \sqrt{3RT} \hookleftarrow \frac{1}{\epsilon} \cdot \tag{25}$$

Here, and in the following, the symbol $\hookleftarrow$ denotes the assignment operator.

In the limit $\epsilon \searrow 0$, the incompressible continuum is reached, since Kn and Ma tend to zero while Re remains constant [48]. Based on that, we assign

$$\bar{c} = \sqrt{\frac{8 k_{\mathrm{B}} T}{m\pi}} \hookleftarrow \sqrt{\frac{8}{3\pi}} \frac{1}{\epsilon} \cdot \tag{26}$$

Further,

$$l_{\mathrm{f}} \hookleftarrow \sqrt{\frac{24}{\pi}} \nu \epsilon \tag{27}$$

and (26) unfold the relaxation time

$$\tau = \frac{l_{\mathrm{f}}}{\bar{c}} \hookleftarrow 3\nu\epsilon^2 \cdot \tag{28}$$

Definition 6. Consequently, we define the ϵ-parametrized BGKBE (17) as

$$\frac{\mathrm{D}}{\mathrm{D}t} f = -\frac{1}{3\nu\epsilon^2} \left(f - M_f^{\mathrm{eq}} \right) \quad \text{in } \mathfrak{R}, \tag{29}$$

where the ϵ-parametrized Maxwellian distribution (12) evaluated at $\left(n_f, \boldsymbol{u}_f \right)$ with (25) is

$$M_f^{\mathrm{eq}} = \frac{n_f \epsilon^d}{\left(\frac{2}{3} \pi \right)^{\frac{d}{2}}} \exp \left(-\frac{3}{2} \left(\boldsymbol{v}\epsilon - \boldsymbol{u}_f \epsilon \right)^2 \right) \quad \text{in } \mathfrak{R}. \tag{30}$$

The BGKBE (29) transforms to

$$f = M_f^{\mathrm{eq}} - 3\nu\epsilon^2 \frac{\mathrm{D}}{\mathrm{D}t} f \quad \text{in } \mathfrak{R}. \tag{31}$$

Repeating $(\mathrm{D}/(\mathrm{D}t))$ (31) gives

$$\frac{\mathrm{D}}{\mathrm{D}t} f = \frac{\mathrm{D}}{\mathrm{D}t} M_f^{\mathrm{eq}} - 3\nu\epsilon^2 \left(\frac{\mathrm{D}}{\mathrm{D}t} \right)^2 f \quad \text{in } \mathfrak{R}. \tag{32}$$

The expression (32) substitutes $(\mathrm{D}/(\mathrm{D}t))f$ in (31). Thus

$$f = M_f^{\mathrm{eq}} - 3\nu\epsilon^2 \frac{\mathrm{D}}{\mathrm{D}t} M_f^{\mathrm{eq}} + \left(3\nu\epsilon^2 \frac{\mathrm{D}}{\mathrm{D}t} \right)^2 f \quad \text{in } \mathfrak{R}. \tag{33}$$

Subsequent repetition produces higher-order terms and substitutions. The appearing power series in ϵ around t reads

$$f = \sum_{i=0}^{\infty} \left(-3\nu\epsilon^2 \frac{\mathrm{D}}{\mathrm{D}t} \right)^i M_f^{\mathrm{eq}} \quad \text{in } \mathfrak{R}. \tag{34}$$

Remark 5. Up to lower order, equation (34) can also be obtained via Maxwell iteration [62] and references therein. The derivation in [62] is however based on an initial Taylor expansion of the material derivative, whereas the present formulation starts with repeated application of the material derivative. Further, similarities to classical Chapman–Enskog expansion (see *e.g.* [61] and references therein) are present. Comparisons of several expansion techniques for a discretized model based on the BGKBE can be found, for example, in [12].

2.3.3. Step 3: Newton's hypothesis

For a solution $f^\star$ of (17) the remaining stress tensor $\mathbf{P}_{f^\star}$ in (20) has to fulfill Newton's hypothesis

$$\mathbf{P}_{f^\star} \stackrel{!}{=} -p_{f^\star}\mathbf{I}_d + 2\nu\rho\mathbf{D}_{f^\star} + \mathcal{O}\left(\epsilon^b\right) \quad \text{in } I \times \Omega \tag{35}$$

up to order $b > 0$, where the rate of strain is denoted by

$$\mathbf{D}_f = \frac{1}{2}\left[\boldsymbol{\nabla}_{\boldsymbol{x}}\boldsymbol{u}_f + \left(\boldsymbol{\nabla}_{\boldsymbol{x}}\boldsymbol{u}_f\right)^{\mathrm{T}}\right]. \tag{36}$$

Proposition 1. *With a cutoff at order $b = 2$ we formally obtain*

$$\mathbf{P} = p\mathbf{I}_d - 2\nu\rho\mathbf{D}. \tag{37}$$

Proof. Equation (34), provides an ansatz

$$f^\star = M_{f^\star}^{\mathrm{eq}} - 3\nu\epsilon^2 \frac{\mathrm{D}}{\mathrm{D}t} M_{f^\star}^{\mathrm{eq}} \quad \text{in } \mathfrak{R}. \tag{38}$$

Due to the assumption that for $\epsilon \searrow 0$ higher order terms become sufficiently small, the order b is large enough. To validate (35), the stress tensor is computed by its definition (8). Unless stated otherwise, f-indices at moments are omitted below. First, the material derivative and (18) is used to obtain

$$\begin{aligned}
\frac{\mathrm{D}}{\mathrm{D}t} M_f^{\mathrm{eq}} &= \left(\frac{1}{\rho}\frac{\mathrm{D}}{\mathrm{D}t}\rho + 3\epsilon^2 \boldsymbol{c}\cdot\frac{\mathrm{D}}{\mathrm{D}t}\boldsymbol{u} - \frac{3\epsilon^2}{m}\boldsymbol{c}\cdot\boldsymbol{F} \right) M_f^{\mathrm{eq}} \\
&= \left[\frac{1}{\rho}\left(\partial_t + \boldsymbol{v}\cdot\boldsymbol{\nabla}_{\boldsymbol{x}}\right)\rho + 3\epsilon^2\boldsymbol{c}\cdot\left(\partial_t + \boldsymbol{v}\cdot\boldsymbol{\nabla}_{\boldsymbol{x}}\right)\boldsymbol{u} - \frac{3\epsilon^2}{m}\boldsymbol{c}\cdot\boldsymbol{F} \right] M_f^{\mathrm{eq}} \\
&= \left[\frac{1}{\rho}\left(-\boldsymbol{u}\cdot\boldsymbol{\nabla}_{\boldsymbol{x}}\rho - \rho\boldsymbol{\nabla}_{\boldsymbol{x}}\cdot\boldsymbol{u} + \boldsymbol{v}\cdot\boldsymbol{\nabla}_{\boldsymbol{x}}\rho\right) + 3\epsilon^2\boldsymbol{c}\cdot\left(\partial_t + \boldsymbol{v}\cdot\boldsymbol{\nabla}_{\boldsymbol{x}}\right)\boldsymbol{u} - \frac{3\epsilon^2}{m}\boldsymbol{c}\cdot\boldsymbol{F} \right] M_f^{\mathrm{eq}} \\
&= \Bigg[-\underbrace{\boldsymbol{\nabla}_{\boldsymbol{x}}\cdot\boldsymbol{u}}_{=:\, a_f} + \underbrace{\frac{\boldsymbol{c}}{\rho}\cdot\boldsymbol{\nabla}_{\boldsymbol{x}}\rho}_{=:\, b_f} + \underbrace{3\epsilon^2\boldsymbol{c}\cdot\partial_t\boldsymbol{u}}_{=:\, c_f} + \underbrace{3\epsilon^2\boldsymbol{c}\cdot\left(\boldsymbol{v}\cdot\boldsymbol{\nabla}_{\boldsymbol{x}}\right)\boldsymbol{u}}_{=:\, d_f} - \underbrace{\frac{3\epsilon^2\boldsymbol{c}}{m}\cdot\boldsymbol{F}}_{=:\, e_f} \Bigg] M_f^{\mathrm{eq}}
\end{aligned} \tag{39}$$

in $\mathfrak{R}$, where $\boldsymbol{c} \coloneqq \boldsymbol{v} - \boldsymbol{u}$ defines the relative velocity. Plugging the derivative (39) into (38) gives

$$f = M_f^{\mathrm{eq}}\left[1 - 3\epsilon^2\nu\left(-a_f + b_f + c_f + d_f + e_f\right)\right] \quad \text{in } \mathfrak{R}. \tag{40}$$

Second, the velocity integrals of terms $a_f, b_f, \dots, e_f$ are individually evaluated. We use the symmetry of M_f^{eq} and that M_f^{eq}/n is a normal distribution with covariance $1/(3\epsilon^2)\mathbf{I}_d$. In $I \times \Omega$ and for any $i, j, k, l \in \{1, 2, ..., d\}$ holds

$$m \int_{\mathbb{R}^d} c_i c_j M_f^{\mathrm{eq}} \,\mathrm{d}\boldsymbol{v} = \frac{\rho}{3\epsilon^2} \delta_{ij}, \tag{41}$$

$$m \int_{\mathbb{R}^d} c_i c_j c_k M_f^{\mathrm{eq}} \,\mathrm{d}\boldsymbol{v} = 0, \tag{42}$$

$$m \int_{\mathbb{R}^d} c_i c_j c_k v_l M_f^{\mathrm{eq}} \,\mathrm{d}\boldsymbol{v} = \frac{\rho}{9\epsilon^4} \Big(\delta_{ij}\delta_{kl} + \delta_{ik}\delta_{jl} + \delta_{il}\delta_{jk} \Big). \tag{43}$$

Hence, we obtain

$$m \int_{\mathbb{R}^d} c_i c_j a_f M_f^{\mathrm{eq}} \,\mathrm{d}\boldsymbol{v} = \left(m \int_{\mathbb{R}^d} c_i c_j M_f^{\mathrm{eq}} \,\mathrm{d}\boldsymbol{v} \right) \partial_{x_k} u_k \overset{(41)}{=} \frac{\rho}{3\epsilon^2} \partial_{x_k} \boldsymbol{u}_k, \tag{44}$$

$$m \int_{\mathbb{R}^d} c_i c_j b_f M_f^{\mathrm{eq}} \,\mathrm{d}\boldsymbol{v} = \left(m \int_{\mathbb{R}^d} c_i c_j c_k M_f^{\mathrm{eq}} \,\mathrm{d}\boldsymbol{v} \right) \frac{1}{\rho} \partial_{x_k} \rho \overset{(42)}{=} 0, \tag{45}$$

$$m \int_{\mathbb{R}^d} c_i c_j c_f M_f^{\mathrm{eq}} \,\mathrm{d}\boldsymbol{v} = \left(m \int_{\mathbb{R}^d} c_i c_j c_k M_f^{\mathrm{eq}} \,\mathrm{d}\boldsymbol{v} \right) 3\epsilon^2 \partial_t u_k \overset{(42)}{=} 0, \tag{46}$$

$$\begin{aligned} m \int_{\mathbb{R}^d} c_i c_j d_f M_f^{\mathrm{eq}} \,\mathrm{d}\boldsymbol{v} &= \left(m \int_{\mathbb{R}^d} c_i c_j c_k v_l M_f^{\mathrm{eq}} \,\mathrm{d}\boldsymbol{v} \right) 3\epsilon^2 \partial_{x_l} u_k \\ &\overset{(43)}{=} \frac{\rho}{3\epsilon^2} \left(\delta_{ij}\delta_{kl} + \delta_{ik}\delta_{jl} + \delta_{il}\delta_{jk} \right) \partial_{x_l} u_k, \end{aligned} \tag{47}$$

$$m \int_{\mathbb{R}^d} c_i c_j e_f M_f^{\mathrm{eq}} \,\mathrm{d}\boldsymbol{v} = \left(m \int_{\mathbb{R}^d} c_i c_j c_k M_f^{\mathrm{eq}} \,\mathrm{d}\boldsymbol{v} \right) \frac{3\epsilon^2}{m} F_k \overset{(42)}{=} 0. \tag{48}$$

Third, for any $i, j \in \{1, 2, ..., d\}$, the component $P_{ij} \coloneqq (\mathbf{P})_{i,j}$ can be computed in $\mathfrak{R}$. Reordering its terms, we achieve

$$\begin{aligned} P_{ij} &= m \int_{\mathbb{R}^d} c_i c_j \left[1 - 3\nu\epsilon^2 \Big(-a_f + b_f + c_f + d_f + e_f \Big) \right] M_f^{\mathrm{eq}} \,\mathrm{d}\boldsymbol{v} \\ &= p\delta_{ij} - 3\nu\epsilon^2 \left[-\frac{\rho}{3\epsilon^2} \partial_{x_k} u_k + \partial_{x_l} u_k \frac{\rho}{3\epsilon^2} \Big(\delta_{ij}\delta_{kl} + \delta_{ik}\delta_{jl} + \delta_{il}\delta_{jk} \Big) \right] \\ &= p\delta_{ij} + \nu\rho \left[\delta_{ij} \partial_{x_k} u_k - \partial_{x_l} u_k \Big(\delta_{ij}\delta_{kl} + \delta_{ik}\delta_{jl} + \delta_{il}\delta_{jk} \Big) \right] \\ &= p\delta_{ij} - \nu\rho \Big(\partial_{x_i} u_j + \partial_{x_j} u_i \Big), \end{aligned} \tag{49}$$

which proves the claim. □

Remark 6. Extending the formal result, the vanishing of higher order terms in the hydrodynamic limit $\epsilon \searrow 0$ is rigorously proven in [48] (Notation: ε instead of ϵ) for the case $\Omega = \mathbb{R}^3$ and initial condition

$$f_\epsilon(0, \boldsymbol{x}, \boldsymbol{v}) = M\left(1 + \epsilon g_\epsilon^0(\boldsymbol{x}, \boldsymbol{v})\right) \tag{50}$$

close to an absolute equilibrium

$$M(\boldsymbol{v}) = \frac{1}{(2\pi)^{d/2}} \exp\left(-\frac{|\boldsymbol{v}|^2}{2}\right) \tag{51}$$

with $\boldsymbol{u}_f = \mathbf{0}$, and $\rho_f = 1 = RT$ and initial fluctuations g_ϵ^0. There, solutions f_ϵ to the ϵ-scaled BGKBE are passed to the limit, where the corresponding velocity moments $\boldsymbol{u}_{f_\epsilon}$ are consequently identified as limiting to Leray's weak solutions [39] of the incompressible NSE [48] (Theorem 1.2). The main result of [48] is transferred to the present setting in Appendix B. It should be noted that we adapted the initial wording "hydrodynamic limit" from [48] to the more generic term "diffusive limit" to underline the presence of diffusion terms in the limiting equation. Hence, we use the terms "diffusive limit/scaling" as generalizations of "hydrodynamic limit/scaling" in an abstract sense, since our methodology is applicable to any PDE that is approximated with LBMs. For example, Simonis [49] applied limit consistency to prove the convergence of LBMs with single and multiple relaxation times to advection–diffusion equations.

Anticipating the discretization of velocity, space and time, we explicitly state the ϵ-parametrized continuous BGKBE in terms of a family of differential equations.

Definition 7. With $\epsilon^2 \times$ (29), we construct the family of BGKBEs

$$\mathcal{F} := \left(\epsilon^2 \frac{\mathrm{D}}{\mathrm{D}t} f^\epsilon + \frac{1}{3\nu}\left(f^\epsilon - M_{f^\epsilon}^{\mathrm{eq}}\right) = 0 \quad \text{in } \mathfrak{R}\right)_{\epsilon > 0}, \tag{52}$$

where the conservable f^ϵ in (52) now displays an upper index ϵ to stress the dependence on the artificial parametrization.

3. Numerical methodology

3.1. Limit consistency

In general, the term consistency is often used to describe a limiting approach for discrete equations to a single continuous one. In the present framework we instead aim to verify conformity of families of equations in terms of weak solution limits under discretization (see Fig. 1). Thus, we adjust the definition of consistency below. The necessity of doing so has been initially motivated in Definition 2.1 in [31]. Further supporting this redefinition, we stress the modular character of the notion of limit consistency. Based on the here proposed methodology, we enable the consistency analysis of discretized kinetic equations in terms of limiting towards a target PDE with a previously imposed parametrization or scaling. We then use this novel methodology to obtain a limit-consistent, intrinsically parallel, discrete evolution equation that forms the centerpiece of many LBMs.

Remark 7. Compared to previous approaches which regard the space-time and velocity discretizations by separate methods, the distinct feature of the present methodology is thus manifested in its generic modularity. Hence, we enable the use of thermodynamic information only if necessary to approximate the model PDE. In particular, in [49] limit consistency is successfully used for analyzing both the convergence of discretized, mathematically abstract relaxation systems without thermodynamic information and the limit information of discretized, BGKBE-based models.

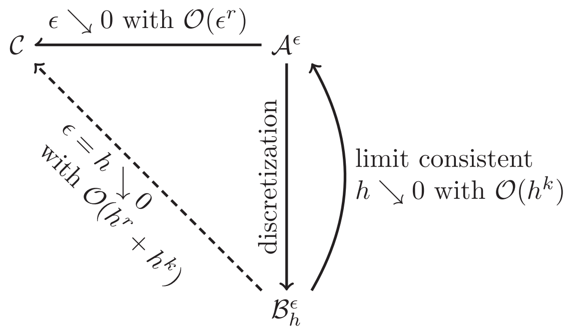

FIGURE 1. Schematic concept of limit consistency. The targeted PDE is denoted with $\mathcal{C}$, the kinetic equation or relaxation system is denoted with $\mathcal{A}^\epsilon$, the kinetic scheme or relaxation scheme is denoted with $\mathcal{B}_h^\epsilon$. The order of approximation (relaxation) in the relaxation parameter ϵ of the relaxation system with respect to the targeted PDE is r. The order of approximation (discretization) in the discretization parameter h of the numerical scheme is k with respect to the relaxation system. The diagonal limit $\mathcal{B}_h^\epsilon \dashrightarrow \mathcal{C}$ for $\epsilon = h \searrow 0$ is presently focused.

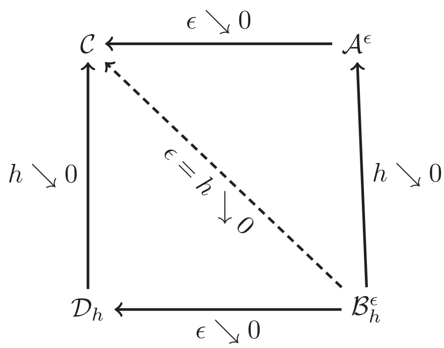

FIGURE 2. Schematic concept of coupled kinetic (relaxation) and discretization limits. The targeted PDE is denoted with $\mathcal{C}$, the kinetic equation or relaxation system is denoted with $\mathcal{A}^\epsilon$, the kinetic scheme or relaxation scheme is denoted with $\mathcal{B}_h^\epsilon$ and the corresponding macroscopic scheme or relaxed scheme is $\mathcal{D}_h$. Here, h defines a velocity or space-time discretization. The diagonal limit $\mathcal{B}_h^\epsilon \dashrightarrow \mathcal{C}$ for $\epsilon = h \searrow 0$ is presently focused.

Remark 8. In order to underline the novelty of the present approach, we compare the idea to established ones with the help of Figure 2. The illustration is based on a given relaxation or kinetic limit $\mathcal{A}^\epsilon \to \mathcal{C}$ for $\epsilon \searrow 0$ from a relaxation system or kinetic equation $\mathcal{A}^\epsilon$ to its targeted PDE $\mathcal{C}$. For example, the well-established property of asymptotic preserving defines whether a stable and consistent space-time discretization $\mathcal{D}_h$ exists in the macroscopic limit $\epsilon \searrow 0$ of a space-time discretized relaxation scheme $\mathcal{B}_h^\epsilon$ [21,24,25]. Here and in the following, $h > 0$ denotes a discretization parameter. In case the discretization is asymptotic preserving, the formal limit equality of equations

$$\lim_{h \searrow 0} \underbrace{\left(\lim_{\epsilon \searrow 0} \mathcal{B}_h^\epsilon \right)}_{= \mathcal{D}_h} \stackrel{!}{=} \lim_{\epsilon \searrow 0} \underbrace{\left(\lim_{h \searrow 0} \mathcal{B}_h^\epsilon \right)}_{= \mathcal{A}^\epsilon} = \mathcal{C} \tag{53}$$

should hold. In contrast to that, here the parameter ϵ is glued to the grid, *i.e.* $\epsilon \leftarrow\!\shortmid h$. Thus, in the context of LBMs, we work with the formal limit equality

$$\lim_{\substack{\epsilon=h \\ h\searrow 0}} \mathcal{B}_h^\epsilon \overset{!}{=} \lim_{\epsilon\searrow 0} \underbrace{\left(\lim_{h\searrow 0} \mathcal{B}_h^\epsilon\right)}_{=\mathcal{A}^\epsilon} = \mathcal{C}, \tag{54}$$

rather than with (53). Drawing the analogy to the limits and continuity of multivariate functions [18] (via $\mathcal{B}_h^\epsilon = \mathcal{B}(\epsilon, h)$), we expect that other shapes of paths than $\epsilon = h$ can be used. In fact, the mapping function $h \leftarrow\!\shortmid \mathcal{O}(\epsilon^{\alpha_0})$ is analyzed in [21]. The overall order α_0 is the minimum of exponents from space $\triangle x$ and time $\triangle t$ discretization in the order of ϵ, respectively, and leads to distinct features of the scheme $\mathcal{B}_h^\epsilon$. Currently, we focus on the order in which the limit point is approximated by the diagonal path ($\epsilon = h$). Notably, hybrid schemes have been derived [30] that are based on a discrete velocity Boltzmann equation and an asymptotic preserving discretization to achieve uniform functionality for all ϵ.

Remark 9. Complementing Remark 8, we explain the main motivation behind our approach. To this end, it is important to recall the differences in taking composed limits of multivariate functions. The situation is nuanced in the sense that a joint limit can lead to outcomes that are different from the ones obtained when taking two subsequent limits. In addition, the result can again be different if the variables are mapped to each other before taking any limit. We illustrate this observation with the following example. Consider a joint limit of $f\colon \mathbb{R}^2 \setminus \{(0,0)\} \to \mathbb{R}$ for $(x, y) \to (0, 0)$. It can be proven that if $\lim_{(x,y)\to(0,0)} f(x, y) = f_0$, then $\lim_{x\to 0} f(x, ax) = f_0$ for all m [18]. Thus, if a scheme $\mathcal{B}_h^\epsilon$ has a limit for $(h, \epsilon) \to (0, 0)$, then this limit must also be reached for mapped parameters $\epsilon \leftarrow\!\shortmid h$. Since we usually assume the case that a limit exists (convergent scheme), the mapped case can be considered as a short cut, since the complexity of the scheme's equations generally reduces from the mapping of parameters. In addition, the negation of this implication is also valuable, since if we cannot find a limit for the mapped parameters, a joint limit does not exist (different results for distinct limit paths that depend on a). Finally, in the practical usage of LBMs, the parameters are usually mapped since we rather want to cross the scales from mesoscopic to macroscopic. This observation is based on the fact that the problems approximated with LBMs mostly contain PDEs describing various phenomena (*e.g.* light transport, waves, turbulence, or solid deformation) on a macroscopic level. In general terms, the most important property of introducing a relaxation to a PDE is that it will vanish once we refine the grid. Specifically in the present context (incompressible flows), keeping the Knudsen number (or Mach number) constant along a refinement of discretization would prevent us from approximating the incompressible NSE. Similarly, a vanishing Mach number for fixed discretization parameters is not a reasonable aim, since it would weaken the robustness and feasibility of the method. In conclusion, we expect that if a scheme is asymptotic preserving, it is also limit consistent. However, from a user perspective, LBMs are known to operate numerically optimally on the mapped parameters along the limit. Hence, it should be regarded as beneficial to be able to decrease the amount of necessary analysis or scheme enhancements from asymptotic preserving towards a minimum required for limit consistency along the specific path of mapped parameters.

Definition 8. Let $d \in \mathbb{N}$ and $X \subseteq \mathbb{R}^d$ with a discretization $X_h \subseteq X$ for any $h \in \mathbb{R}_{>0}$. Let $U(X)$ and $W_h(X_h)$ denote Hilbert spaces on X and X_h, respectively, where W_h contains the grid functions of $\{v_h\colon X_h \to \mathbb{R}\}$. Via

$$\mathcal{A}^\epsilon = \left(A^\epsilon\left(\cdot\right) = 0 \quad \text{in } U\right)_{\epsilon>0}, \tag{55}$$

$$\mathcal{B}_h^\epsilon = \left(B_h^\epsilon\left(\cdot\right) = 0 \quad \text{in } W_h\right)_{\epsilon>0,h>0}, \tag{56}$$

families of PDEs are defined by continuous and discrete operators A^ϵ and B_h^ϵ, respectively. The solutions of instances of (55) and (56) are indicated with $a^\epsilon \in U$ for all $\epsilon > 0$ and $b_h^\epsilon \in W_h$ for all $\epsilon, h > 0$, respectively.

Conforming to Definition 8, we occasionally adopt the notation

$$\mathcal{C} = \left(C\left(\cdot\right) = 0 \quad \text{in } \tilde{U}\right) \tag{57}$$

for a single PDE with a solution c in the Hilbert space $\tilde{U}(X)$.

Definition 9. Let $\mathcal{A}^\epsilon$ and $\mathcal{C}$ be given as in (55) and (57), respectively. The abstracted solution limit of a solution a^ϵ to $\mathcal{A}^\epsilon$ toward a solution c to $\mathcal{C}$ for $\epsilon \searrow 0$ is denoted with

$$a^\epsilon \rightharpoonup c \tag{58}$$

and defines convergence in the broadest sense (*e.g.* formal, weak, or strong). The formal order $r \geq 0$ of this convergence is $A^\epsilon(c) \in \mathcal{O}(\epsilon^r)$. The information of both, the formal PDE convergence and the solution convergence, is compressed in the notation

$$\mathcal{A}^\epsilon \xrightharpoonup[\mathcal{O}(\epsilon^r)]{\epsilon\searrow 0} \mathcal{C}. \tag{59}$$

Based on the abstracted but formally determined background limit in Definition 9, we propose the following specialized notion of consistency.

Definition 10. Let $\mathcal{A}^\epsilon$ admit an abstracted solution limit of order $\mathcal{O}(\epsilon^r)$ in $\epsilon \searrow 0$ to a solution c of a PDE system $\mathcal{C}$ as in Definition 9. Then, $\mathcal{B}_h^\epsilon$ is called limit consistent of order $k > 0$ to $\mathcal{A}^\epsilon$ in $W_h(X_h)$, if for any fixed $\epsilon > 0$ it holds that

– $B_h^\epsilon(a^\epsilon|_{X_h}) \in \mathcal{O}\left(h^k\right)$ in W_h , and
– $k \geq r$.

The residual expression $B_h^\epsilon(a^\epsilon|_{X_h})$ is called truncation error.

Lemma 1. *Let $\mathcal{B}_h^\epsilon$ be limit consistent of order k to $\mathcal{A}^\epsilon$ in $W_h(X_h)$. Then for any fixed $\epsilon > 0$ we have*

$$\left[B_h^\epsilon\Big(a^\epsilon\,|_{X_h}\Big) \in \mathcal{O}\Big(h^k\Big) \quad in\ W_h\right] \iff \lim_{h\searrow 0}\sup_{x\in X_h}\left|\frac{B_h^\epsilon\Big(a^\epsilon|_{X_h}\Big)(x)}{h^k}\right| < \infty. \tag{60}$$

Proof. We interpret the operation

$$\cdot\Big|_{X_h} : U \to W_h, f \mapsto f\Big|_{X_h} \tag{61}$$

as an interpolation which is exact at the grid nodes of X_h. Let $\epsilon > 0$ be fixed. Forming the local truncation error of B_h^ϵ with respect to A^ϵ, via insertion of the exact solution a^ϵ evaluated at the grid nodes [40], gives

$$B_h^\epsilon\big(a^\epsilon|_{X_h}\big) = Kh^k + \mathcal{O}\big(h^{k+1}\big), \tag{62}$$

with a constant $K < \infty$. Due to consistency, *i.e.* the local truncation nulling out for $h \searrow 0$, we can limit

$$\lim_{h\searrow 0}\left\|B_h^\epsilon\big(a^\epsilon|_{X_h}\big)\right\| = 0, \tag{63}$$

where $\|\cdot\| \coloneqq \sup_{x\in X_h}|\cdot|$ defines a supremum norm on W_h. Similarly, we have that

$$\lim_{h\searrow 0}\left\|\frac{B_h^\epsilon\left(a^\epsilon|_{X_h}\right)}{h^k}\right\| = \lim_{h\searrow 0}\left\|\frac{Kh^k + \mathcal{O}\left(h^{k+1}\right)}{h^k}\right\| = K + \mathcal{O}(1) < \infty. \tag{64}$$

□

Remark 10. It is to be stressed that the difference to classical consistency is with respect to the exact solution a^ϵ being already parametrized in ϵ. Via the assignment of the artificial parameter $\epsilon \hookleftarrow h$ and the interpolation $a^{\epsilon \hookleftarrow h}|_{X_h}$ onto the grid nodes, the kinetic/relaxation parametrization is irreversibly coupled to the discretization. The process of discretization has thus to be consistent with or at least uphold this limit. If this is the case, the limit consistency implies classical consistency for the special case of mapped relaxation and discretization parameters and with concatenated orders.

Remark 11. Note that in Definition 10, we have purposely not specified the limit $\mathcal{A}^\epsilon \xrightarrow{\epsilon \searrow 0} \mathcal{C}$ further. Dependent on the situation at hand, this limit can be *e.g.* weak or strong. For example, the former is the case when approximating weak solutions of the incompressible NSE (1) with the BGKBE (17) [48] in diffusive scaling. The latter is given when using a relaxation system (or the corresponding BGK model [53]), for the approximation of scalar, linear, d-dimensional ADE [56]. The limit can also be in terms of unique entropy solutions if $\boldsymbol{F}$ is nonlinear [10].

Remark 12. By Lemma 1, we have identified $B_h^\epsilon(a^\epsilon|_{X_h})$ as the abstracted local truncation error

$$-T_h^\epsilon \coloneqq \underbrace{B_h^\epsilon\left(b_h^\epsilon\right)}_{=0} - B_h^\epsilon\left(a^\epsilon|_{X_h}\right) \tag{65}$$

(*e.g.* see [5, 40]) with an additional relaxation limit running in the background. As a consequence, demanding stability seems natural to complete the convergence result.

Let the global error be defined by

$$E_h^\epsilon = b_h^\epsilon - a^\epsilon|_{X_h}. \tag{66}$$

We cutoff the Taylor expansion of $B_h^\epsilon(b_h^\epsilon)$ at $a^\epsilon|_{X_h}$ given by

$$B_h^\epsilon\left(b_h^\epsilon\right) = \sum_{n=0}^{\infty} \frac{1}{n!}\left(\partial_{b_h^\epsilon}\right)^n B_h^\epsilon\left(a^\epsilon|_{X_h}\right)\left(E_h^\epsilon\right)^n \tag{67}$$

to obtain a linearized expression

$$J_{B_h^\epsilon}\left(a^\epsilon|_{X_h}\right)E_h^\epsilon = -T_h^\epsilon + \mathcal{O}\left(\|E_h^\epsilon\|^2\right), \tag{68}$$

where $J_{B_h^\epsilon}(a^\epsilon|_{X_h})$ denotes the Jacobian of the discrete operator B_h^ϵ at exact solutions a^ϵ of A^ϵ evaluated on the grid. The nonlinear terms are gathered in $\mathcal{O}\big(\|E_h^\epsilon\|^2\big)$. Following [40] we can define a notion of stability with respect to the linearized discretization.

Definition 11. For fixed ϵ, the linearized discrete operator B_h^ϵ is stable in some norm $\|\cdot\|_{W_h}$ on W_h if its inverse Jacobian at the exact solution evaluated at X_h is uniformly bounded for $h \searrow 0$ in the sense that there exist constants $K > 0$ and h_0 such that

$$\left\|\left(J_{B_h^\epsilon}\left(a^\epsilon|_{X_h}\right)\right)^{-1}\right\| \leq K \quad \text{for all } h < h_0. \tag{69}$$

Remark 13. In the context of the LBM, where B_h^ϵ is the (space-time-velocity discrete) LBE for $\epsilon \hookleftarrow h$, several previous works derived bounds for linearized amplification matrices in the sense of von Neumann (*e.g.* [53]) and proved weighted L^2-stability [27] for linearized collisions which admit a stability structure. In fact, non-linear stability estimates for LBMs naturally involve the notion of entropy in a mathematical (relaxation) [11] or thermodynamical (dynamical system) [9] sense.

Remark 14. Upon the condition that the lattice Boltzmann discretizations are stable in some norm, limit consistency can be used to infer classical consistency, and hence convergence [40, 58] toward the target PDE. Below, the general notion of convergence is to be understood in terms of the kind of relaxation or kinetic background limit $\mathcal{A}^\epsilon \xrightarrow{\epsilon\searrow 0} \mathcal{C}$ only (*e.g.* formal, weak, or strong).

Lemma 2. *Let $\mathcal{A}_h^\epsilon$ and $\mathcal{B}_h^\epsilon$ be given as in Definition 10 and let*

– *$\mathcal{B}_h^\epsilon$ be limit consistent of order k to $\mathcal{A}^\epsilon$,*
– *B_h^ϵ be stable and linear in the terms of Definition 11.*

Then we obtain an overall convergence result of solutions in the sense of

$$\mathcal{B}_h^\epsilon \xrightarrow[\mathcal{O}(\epsilon^r)|_{X_h}+\mathcal{O}(\epsilon^k)]{(\epsilon,h)\searrow(0,0)} \mathcal{C} \equiv \left(\mathcal{A}^\epsilon \xrightarrow[\mathcal{O}(\epsilon^r)]{\epsilon\searrow 0} \mathcal{C}\right) \circ \left(\mathcal{B}_h^\epsilon \xrightarrow[\mathcal{O}(h^k)]{h\searrow 0} \mathcal{A}^\epsilon\right), \tag{70}$$

where the symbol $\equiv$ denotes arrow equality irrespective of the nature of the mappings. Furthermore, if $\epsilon = \iota(h)$ via $\iota = \mathrm{id}$, b_h^ϵ converges at the order r to c.

Proof. For fixed $\epsilon > 0$, limit consistency of $\mathcal{B}_h^\epsilon$ and the stability of B_h^ϵ imply classically [38] that

$$\begin{aligned} \left\|E_h^\epsilon\right\| &= \left\|-\left(J_{B_h^\epsilon}\left(a^\epsilon|_{X_h}\right)\right)^{-1} T_h^\epsilon + \mathcal{O}\left(\left\|E_h^\epsilon\right\|^2\right)\right\| \\ &\le \left\|\left(J_{B_h^\epsilon}\left(a^\epsilon|_{X_h}\right)\right)^{-1}\right\| \left\|T_h^\epsilon\right\| \\ &\le K\mathcal{O}\big(h^k\big) \end{aligned} \tag{71}$$

and hence

$$b_h^\epsilon = a^\epsilon|_{X_h} + \mathcal{O}\big(h^k\big). \tag{72}$$

Similarly, from the background (relaxation or kinetic) limit, we have that

$$a^\epsilon = c + \mathcal{O}\left(\epsilon^r\right). \tag{73}$$

Combining (72) and (73) we obtain

$$b_h^\epsilon = c|_{X_h} + \mathcal{O}\left(\epsilon^r\right)|_{X_h} + \mathcal{O}\left(h^k\right). \tag{74}$$

Now let $\epsilon \leftarrow\!\!\shortmid \iota(h)$. Thus, since $\mathcal{O}(\epsilon^r)|_{X_h}$ are higher order terms interpolated on the grid nodes, we see that their leading order in h is r. Conclusively, (74) becomes

$$\begin{aligned} b_h^\epsilon &= c|_{X_h} + \mathcal{O}\Big(\iota(h)^r + h^k\Big) \\ &= c|_{X_h} + \mathcal{O}\left(h^{\min\{r,k\}}\right) \\ &= c|_{X_h} + \mathcal{O}\left(h^r\right), \end{aligned} \tag{75}$$

due to the limit-consistent discretization. □

Remark 15. Having established the definition of limit consistency, we utilize it below to provide limit-consistent discretizations of families of BGK Boltzmann equations, as suggested in Figure 3. In particular, we elaborate on the previous work of Krause [31] by reconstructing the discretizations and validating the procedure in terms of limit consistency.

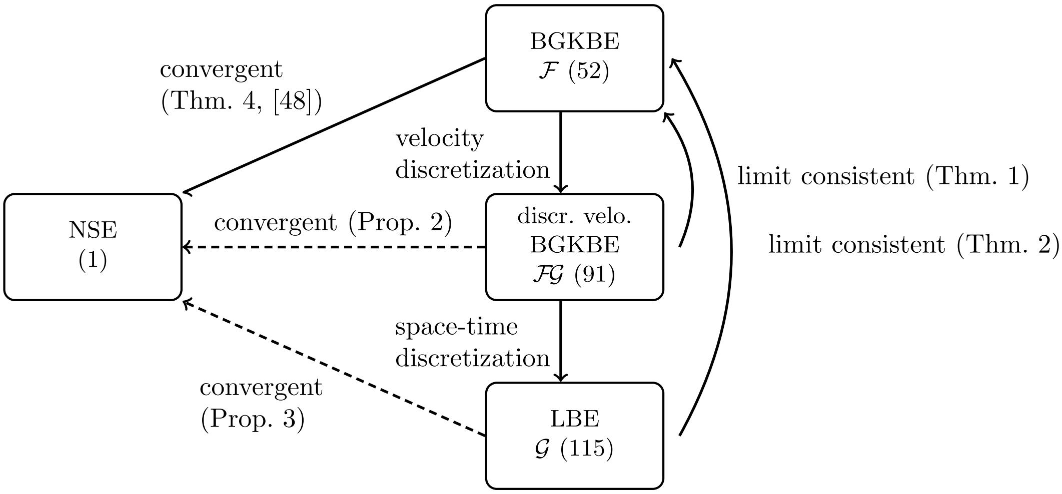

FIGURE 3. Illustration of limit consistency as it is applied in the present setting.

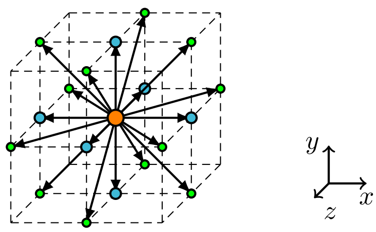

FIGURE 4. The $D3Q19$ discrete velocity set. Coloring refers to energy shells: orange, cyan, green denote zeroth, first, second order, respectively. Figure from [49].

Remark 16. It is to be noted that the above statements are made for an abstracted convergence notion (formal, weak, or strong), specifically, Definition 9, Definition 10, Lemma 1, Lemma 2. Thus, we distinguish between formal, weak, and strong convergence of the underlying kinetic limit. Based on the respective type of this underlying limit, all our additional derivations are at most of the same rigor. For example, (73) is to be understood in this abstract sense. If the order of convergence is known to be $\mathcal{O}(\epsilon^r)$, (73) is valid for all the cases in the same respective sense. In the case of a formal limit, the convergence order is given directly, and all derived results are only formal, as well. In the case of a weak limit without any further regularity assumption, we can generally deduce a formal limit only. However, given, for example, sufficient smoothness in ϵ, see Appendix A.2, we can transition to a weak concatenated limit. In the case of a strong limit, the norm bound implies that an asymptotic expansion such as (73) is well-defined. More specifically, the fact that $a^\epsilon \xrightarrow[w]{\epsilon\searrow 0} c$ implies $\|c\| \leq \liminf_{\epsilon\searrow 0} \|a^\epsilon\|$ provides the validity of (73) if the convergence order is given to be $\mathcal{O}(\epsilon^r)$ in some sense (see Appendix A.2).

3.2. Discretization of velocity

Classically, the discrete velocity BGKBE is a result of reducing the velocity space Ξ of the BGKBE (17) to a countable finite set. Let $\epsilon \in \mathbb{R}_{>0}$ and ν be fixed and define the set $Q = \{\boldsymbol{v}_i \mid i = 0, 1, \ldots, q-1\} \subseteq \Xi = \mathbb{R}^d$, which is countable and finite with $q := \#Q < \infty$. Below, we regularly denote Q as $DdQq$ instead.

Unless stated otherwise, in the present work we use $Q = D3Q19$ which is depicted in Figure 4 and defined as follows.

Definition 12. The $D3Q19$ stencil is defined through its elements

$$\mathbb{R}^3 \ni \boldsymbol{v}_i = \frac{1}{\epsilon} \begin{cases} (0,0,0)^{\mathrm{T}} & \text{if } i = 0, \\ (\pm 1,0,0)^{\mathrm{T}}, (0,\pm 1,0)^{\mathrm{T}}, (0,0,\pm 1)^{\mathrm{T}} & \text{if } i = 1,2,\dots,6, \\ (0,\pm 1,\pm 1)^{\mathrm{T}}, (\pm 1,\pm 1,0)^{\mathrm{T}}, (\pm 1,0,\pm 1)^{\mathrm{T}} & \text{if } i = 7,8,\dots,18, \end{cases} \tag{76}$$

distributed on three energy shells [29].

In the following, we assume that a solution f^ϵ to (29) exists and is integrable to well-defined hydrodynamic moments n_{f^ϵ} and $\boldsymbol{u}_{f^h}$. The dependence of f^ϵ on ϵ transfers to its moments, such that $n_{f^\epsilon}, \boldsymbol{u}_{f^\epsilon} \in \mathcal{O}(1)$ is not assumed, but holds by construction instead. Taylor expanding $M^{\mathrm{eq}}_{f^\epsilon}(t,\boldsymbol{x},\boldsymbol{v}_i)$ in ϵ such that in $I \times \Omega \times Q$ a separation at order two yields

$$\begin{aligned} M^{\mathrm{eq}}_{f^\epsilon}(t,\boldsymbol{x},\boldsymbol{v}_i) &= \frac{n_{f^\epsilon}\epsilon^d}{\left(\frac{2}{3}\pi\right)^{\frac{d}{2}}} \exp\left(-\frac{3}{2}\widetilde{\boldsymbol{v}}_i^2\right) \exp\left(3\epsilon\widetilde{\boldsymbol{v}}_i \cdot \boldsymbol{u}_{f^\epsilon} - \frac{3}{2}\epsilon^2 \boldsymbol{u}_{f^\epsilon}^2\right) \\ &= \underbrace{\frac{n_{f^\epsilon}\epsilon^d}{\left(\frac{2}{3}\pi\right)^{\frac{d}{2}}} \exp\left(-\frac{3}{2}\widetilde{\boldsymbol{v}}_i^2\right) \left[1 + 3\epsilon\widetilde{\boldsymbol{v}}_i \cdot \boldsymbol{u}_{f^\epsilon} - \frac{3}{2}\epsilon^2\boldsymbol{u}_{f^\epsilon}^2 + \frac{9}{2}\epsilon^2\left(\widetilde{\boldsymbol{v}}_i \cdot \boldsymbol{u}_{f^\epsilon}\right)^2\right]}_{=:\ \widetilde{M}^{\mathrm{eq}}_{f^\epsilon}} \\ &\quad + R^{(0)}_{t,\boldsymbol{x},\boldsymbol{v}_i}, \end{aligned} \tag{77}$$

where $R^{(0)}_{t,\boldsymbol{x},\boldsymbol{v}_i} \in \mathcal{O}(\epsilon^{d+3})$ defines a remainder term for any $(t,\boldsymbol{x},\boldsymbol{v}_i) \in I \times \Omega \times Q$. Where unambiguous, we drop the corresponding indexes below. Note that the prefactorization $\widetilde{\boldsymbol{v}}_i := \epsilon\boldsymbol{v}_i$ removes the ϵ-dependence. To uphold conservation properties inherited by the evaluated Maxwellian distribution $M^{\mathrm{eq}}_{f^\epsilon}$ we introduce the weights $w_i \in \mathbb{R}_{>0}$ for $i = 0,1,\dots,q-1$ such that in $I \times \Omega$

$$n_{f^\epsilon} = \sum_{i=0}^{q-1} w_i \widetilde{M}^{\mathrm{eq}}_{f^\epsilon}, \tag{78}$$

$$n_{f^\epsilon}\boldsymbol{u}_{f^\epsilon} = \sum_{i=0}^{q-1} w_i \boldsymbol{v}_i \widetilde{M}^{\mathrm{eq}}_{f^\epsilon}. \tag{79}$$

Using Gauss–Hermite quadrature the weights w_i for $D3Q19$ are deduced as

$$w_i = w \begin{cases} \frac{1}{3} & \text{if } i = 0, \\ \frac{1}{18} & \text{if } i = 1,2,\dots,6, \\ \frac{1}{36} & \text{if } i = 7,8,\dots,18, \end{cases} \tag{80}$$

where

$$w\left(\tilde{\boldsymbol{v}}_i\right) := \left(\frac{2}{3}\pi\right)^{\frac{d}{2}} \epsilon^{-d} \exp\left(\frac{3}{2}\widetilde{\boldsymbol{v}}_i^2\right). \tag{81}$$

Lemma 3. *With the above, the integral moments of f^ϵ are approximated in $I \times \Omega$ by sums over the discrete velocities. In particular, for zeroth and first order this gives*

$$n_{f^\epsilon} - \sum_{i=0}^{q-1} w_i f^\epsilon \in \mathcal{O}\left(\epsilon^2\right), \tag{82}$$

$$\boldsymbol{u}_{f^\epsilon} - \frac{\sum_{i=0}^{q-1} w_i \boldsymbol{v}_i f^\epsilon}{\sum_{i=0}^{q-1} w_i f^\epsilon} \in \mathcal{O}(\epsilon). \tag{83}$$

Proof. In $I \times \Omega$ we can classify

$$\begin{aligned}\int_{\mathbb{R}^d} f^\epsilon \,\mathrm{d}\boldsymbol{v} = n_{f^\epsilon} = \sum_{i=0}^{q-1} w_i \widetilde{M}^{\mathrm{eq}}_{f^\epsilon} &= \sum_{i=0}^{q-1} w_i M^{\mathrm{eq}}_{f^\epsilon} + R^{(1)}_{t,\boldsymbol{x}} \\ &= \sum_{i=0}^{q-1} w_i \left(f^\epsilon + 3\nu\epsilon^2 \frac{\mathrm{D}}{\mathrm{D}t} f^\epsilon \right) + R^{(1)}_{t,\boldsymbol{x}} \\ &= \sum_{i=0}^{q-1} w_i f^\epsilon + R^{(2)}_{t,\boldsymbol{x}}\end{aligned} \tag{84}$$

and

$$\begin{aligned}\int_{\mathbb{R}^d} \boldsymbol{v} f^\epsilon \,\mathrm{d}\boldsymbol{v} = n_{f^\epsilon} \boldsymbol{u}_{f^\epsilon} = \sum_{i=0}^{q-1} w_i \boldsymbol{v}_i \widetilde{M}^{\mathrm{eq}}_{f^\epsilon} &= \sum_{i=0}^{q-1} w_i \boldsymbol{v}_i M^{\mathrm{eq}}_{f^\epsilon} + R^{(3)}_{t,\boldsymbol{x}} \\ &= \sum_{i=0}^{q-1} w_i \boldsymbol{v}_i \left(f^\epsilon + 3\nu\epsilon^2 \frac{\mathrm{D}}{\mathrm{D}t} f^\epsilon \right) + R^{(3)}_{t,\boldsymbol{x}} \\ &= \sum_{i=0}^{q-1} \left(w_i \boldsymbol{v}_i f^\epsilon \right) + R^{(4)}_{t,\boldsymbol{x}},\end{aligned} \tag{85}$$

respectively. We categorize the remainder terms $R^{(\cdot)}_{\cdot,\cdot}$ as follows. For all $i = 0, 1, ..., q-1$, the weight w_i defined in (80) is seen as a function of ϵ in the sense of (81) such that $w_i \in \mathcal{O}(\epsilon^{-d})$. Thus, the product $w_i(\mathrm{D}/(\mathrm{D}t)) f^\epsilon(t, \boldsymbol{x}, \boldsymbol{v}_i)$ is also a function of ϵ and hence in $\mathcal{O}(1)$ for all $(t, \boldsymbol{x}, \boldsymbol{v}_i) \in I \times \Omega \times Q$. Further, recall from (77) that $M^{\mathrm{eq}}_{f^\epsilon}$ is approximated by $\widetilde{M}^{\mathrm{eq}}_{f^\epsilon}$ with an error in $\mathcal{O}(\epsilon^{3+d})$ for all $(t, \boldsymbol{x}, \boldsymbol{v}_i) \in I \times \Omega \times Q$. Henceforth, with $\boldsymbol{v}_i \in \mathcal{O}(\epsilon^{-1})$ by construction, we obtain for all $(t, \boldsymbol{x}) \in I \times \Omega$ that

- $R^{(1)}_{t,\boldsymbol{x}} \in \mathcal{O}(\epsilon^3)$,
- $R^{(2)}_{t,\boldsymbol{x}} \in \mathcal{O}(\epsilon^2)$,
- $R^{(3)}_{t,\boldsymbol{x}} \in \mathcal{O}(\epsilon^2)$, and
- $R^{(4)}_{t,\boldsymbol{x}} \in \mathcal{O}(\epsilon)$

which completes the proof. ☐

Definition 13. For $i = 0, 1, ..., q-1$ and in $I \times \Omega$ we define

$$f_i^\epsilon(t, \boldsymbol{x}) := w_i f^\epsilon(t, \boldsymbol{x}, \boldsymbol{v}_i), \tag{86}$$

$$n_{\boldsymbol{f}^\epsilon}(t, \boldsymbol{x}) := \sum_{i=0}^{q-1} f_i^\epsilon(t, \boldsymbol{x}), \tag{87}$$

$$\boldsymbol{u}_{\boldsymbol{f}^\epsilon}(t, \boldsymbol{x}) := \frac{1}{n_{\boldsymbol{f}^\epsilon}(t, \boldsymbol{x})} \sum_{i=0}^{q-1} \boldsymbol{v}_i f_i^\epsilon(t, \boldsymbol{x}), \tag{88}$$

$$\overline{M}^{\mathrm{eq}}_{\boldsymbol{f}^{\epsilon},i}(t,\boldsymbol{x}) := \left\{ \frac{w_i}{w} n_{\boldsymbol{f}^{\epsilon}} \left[1 + 3\epsilon^2 \boldsymbol{v}_i \cdot \boldsymbol{u}_{\boldsymbol{f}^{\epsilon}} - \frac{3}{2}\epsilon^2 \boldsymbol{u}^2_{\boldsymbol{f}^{\epsilon}} + \frac{9}{2}\epsilon^4 \left(\boldsymbol{v}_i \cdot \boldsymbol{u}_{\boldsymbol{f}^{\epsilon}}\right)^2 \right] \right\} (t,\boldsymbol{x}). \tag{89}$$

Definition 14. Multiplication $w_i \times$ (29) and injection of Definition 13, we obtain the discrete velocity BGKBE as a system of q equations

$$\frac{\mathrm{D}}{\mathrm{D}t} f_i^{\epsilon} = -\frac{1}{3\nu\epsilon^2} \left(f_i^{\epsilon} - \overline{M}^{\mathrm{eq}}_{\boldsymbol{f}^{\epsilon},i} \right) \quad \text{in } I \times \Omega, \tag{90}$$

for $i = 0, 1, \ldots, q-1$. The upheld parametrization with ϵ generates the family of discrete velocity BGKBE

$$\mathcal{FG} := \left(\frac{\mathrm{D}}{\mathrm{D}t} f_i^{\epsilon} + \frac{1}{3\nu\epsilon^2} \left(f_i^{\epsilon} - \overline{M}^{\mathrm{eq}}_{\boldsymbol{f}^{\epsilon},i} \right) = 0 \quad \text{in } I \times \Omega \times Q \right)_{\epsilon > 0}. \tag{91}$$

Theorem 1. *Suppose that for given $\epsilon, \nu \in \mathbb{R}_{>0}$, f^{ϵ} is a weak solution of the BGKBE (29) with well-defined integral moments $n_{f^{\epsilon}}$ and $\boldsymbol{u}_{f^{\epsilon}}$ and that for $n_{f^{\epsilon}}$, $\boldsymbol{u}_{f^{\epsilon}}$, $w_i \frac{\mathrm{D}}{\mathrm{D}t} f^{\epsilon}$ understood as functions of ϵ holds*

$$n_{f^{\epsilon}} \in \mathcal{O}(1) \quad \text{in } I \times \Omega, \tag{92}$$

$$\boldsymbol{u}_{f^{\epsilon}} \in \mathcal{O}(1) \quad \text{in } I \times \Omega, \tag{93}$$

$$w_i \frac{\mathrm{D}}{\mathrm{D}t} f^{\epsilon} \in \mathcal{O}(1) \quad \text{in } I \times \Omega \times Q. \tag{94}$$

Then, the family $\mathcal{FG}$ of discrete velocity BGKBEs (91) is limit consistent of order two to the family $\mathcal{F}$ of BGKBEs (52) in $I \times \Omega \times Q$.

Proof. As a direct consequence of measuring the remainder terms which gives (82) and (83) in Lemma 3, we obtain the overall truncation error

$$\epsilon^2 \frac{\mathrm{D}}{\mathrm{D}t} f_i^{\epsilon} + \frac{1}{3\nu} \left(f_i^{\epsilon} - \overline{M}^{\mathrm{eq}}_{\boldsymbol{f}^{\epsilon},i} \right) \in \mathcal{O}\left(\epsilon^2\right) \quad \text{in } I \times \Omega \times Q \tag{95}$$

for $i = 0, 1, \ldots, q-1$. Thus, the conditions in Definition 10 are verified at order $k = 2$. □

Proposition 2. *Under the premise of linear stability of velocity discretizations, sufficiently smooth solutions of the family of discrete velocity BGKBEs $\mathcal{FG}$ (91) converge weakly to solutions of the incompressible NSE (1) with second-order limit consistency.*

Proof. To begin with, we derive a convergence order estimate for a velocity solution $\boldsymbol{u}$ of the NSE (1) in terms of the velocity moment $\boldsymbol{u}_{f^{\epsilon}}$ of the BGKBE (17). The motivation is to color the abstract proof of Lemma 2, specifically, to prove that we can obtain a realization of (73) from the weak convergence results of Saint-Raymond [48]. Under the assumption of weak convergence of $\boldsymbol{u}_{f^{\epsilon}}$ toward $\boldsymbol{u}$ (see Theorem 4 for details), we have

$$\mathfrak{I}^{\epsilon} = \int_0^T \int_{\mathbb{R}^d} \phi(t,\boldsymbol{x}) \Big(\boldsymbol{u}_{f^{\epsilon}}(t,\boldsymbol{x}) - u(t,\boldsymbol{x}) \Big) \,\mathrm{d}\boldsymbol{x}\,\mathrm{d}t \to 0 \quad \text{for } \varepsilon \to 0, \tag{96}$$

for some test function ϕ and a fixed time $T \in I$. To match the notation in [48], we reinsert $\tau \leftrightarrow 3\nu\epsilon^2$. From Proposition 1, we have that the Chapman–Enskog expansion

$$u_{f^{\tau}} = u - \tau \frac{1}{\rho_{f^{\tau}}} \boldsymbol{\nabla}_{\boldsymbol{x}} \cdot \boldsymbol{\Pi} + \mathcal{O}(\tau^2), \tag{97}$$

is valid formally in general and rigorously for sufficiently smooth data, where $\boldsymbol{\Pi} = -2\nu\mathbf{D}$ is the viscous stress tensor. With the expansion (97) we obtain

$$\mathfrak{I}^{\tau} = -\tau \int_0^T \int_{\mathbb{R}^d} \frac{1}{\rho_{f^{\tau}}} \phi(t,\boldsymbol{x}) \boldsymbol{\nabla}_{\boldsymbol{x}} \cdot \boldsymbol{\Pi} \,\mathrm{d}\boldsymbol{x}\,\mathrm{d}t + \mathcal{O}(\tau^2). \tag{98}$$

Integration by parts yields

$$\int_0^T \int_{\mathbb{R}^d} \phi \boldsymbol{\nabla}_{\boldsymbol{x}} \cdot \boldsymbol{\Pi} \, \mathrm{d}\boldsymbol{x} \, \mathrm{d}t = - \int_0^T \int_{\mathbb{R}^d} \boldsymbol{\nabla}_{\boldsymbol{x}} \phi \cdot \boldsymbol{\Pi} \, \mathrm{d}\boldsymbol{x} \, \mathrm{d}t. \tag{99}$$

Thus, using Cauchy–Schwarz and approximating $\boldsymbol{\Pi} \approx -2\nu \boldsymbol{\nabla}_{\boldsymbol{x}} \boldsymbol{u}$ from (36), we have

$$\left|\mathfrak{I}^\tau\right| \leq C\tau \left\|\boldsymbol{\nabla}_{\boldsymbol{x}}\phi\right\|_{L^2} \left\|\boldsymbol{\nabla}_{\boldsymbol{x}}\boldsymbol{u}\right\|_{L^2} + \mathcal{O}(\tau^2), \tag{100}$$

with a constant C, since ν and ρ_{f^τ} are bounded (sufficiently smooth solutions). Finally,

$$\int_0^T \int_{\mathbb{R}^d} \phi(t,\boldsymbol{x}) \left(\boldsymbol{u}_{f^\tau} - \boldsymbol{u}\right) \mathrm{d}\boldsymbol{x} \, \mathrm{d}t = \mathcal{O}(\tau). \tag{101}$$

Thus, we have obtained second-order weak convergence in terms of $\mathcal{O}(\tau) = \mathcal{O}(\epsilon^2)$. Since we have achieved the baseline convergence order estimate (73), we can apply Lemma 2. Thus, the convergence of $\mathcal{FG}$ with second order consistent discretization unfolds by

$$\mathcal{FG} \xrightarrow[\mathcal{O}(\epsilon^2)]{\epsilon\searrow 0} \mathrm{NSE} \equiv \left(\mathcal{F} \xrightarrow[\mathcal{O}(\epsilon^2)]{\epsilon\searrow 0} \mathrm{NSE}\right) \circ \left(\mathcal{FG} \xrightarrow[\mathcal{O}(\epsilon^2)]{\epsilon\searrow 0} \mathcal{F}\right). \tag{102}$$

□

3.3. Discretization of space and time

By completion of the discretization, the parameter ϵ is glued to the space-time grid. This procedure resembles the typical connection of relaxation and discretization limit in LBMs [53] to uphold the consistency to the initially targeted NSE (1). In the following, we provide a consistent limit discretization in exactly that sense.

Let Ω be uniformly discretized by a Cartesian grid Ω_h with $N+1$ nodes x per dimensional direction, where h denotes the grid parameter (as abstracted in Fig. 1). For the largest cubic subdomain $\tilde{\Omega}_h \subseteq \Omega_h \subseteq \Omega$ we define $\triangle x = |\tilde{\Omega}_h|^{1/d}/N$. By imposing the spatiotemporal coupling $\triangle t \sim \triangle x^2$, we retain a positioning constraint $v_{i\alpha} = \flat \triangle x/\triangle t$ on the grid nodes for $\flat \in \{0, \pm 1\}$ (up to three shells) and define the discrete time interval $I_{\triangle t} \coloneqq \{t = t_0 + k\triangle t \mid t_0 \in I, k \in \mathbb{N}\} \subseteq I$. Here and below, the continuous ϵ-parametrization is linked with the grid parameters by mapping $\epsilon \leftarrow\!\!\!\mapsto h = \triangle x \sim \sqrt{\triangle t}$.

Definition 15. Let $I_h \times \Omega_h \times Q$ be the discrete version of $\mathfrak{R}$ and be constructed as above. Assume that f^h denotes a solution of BGKBE (29). Continuing from (86), for $i = 0, 1, \ldots, q-1$ and $\chi \in \mathbb{R}$, we define the i-th population

$$f_i^h\left(t + \chi h^2\right) = f_i^h\left(t + \chi h^2, \cdot\right) \coloneqq f_i^h\left(t + \chi h^2, \boldsymbol{x} + \boldsymbol{v}_i \chi h\right) \tag{103}$$

on the space-time cylinder $(t, \boldsymbol{x}) \in I_h \times \Omega_h$.

Below, external forces $\boldsymbol{F} = 0$ are neglected. For the inclusion of forces, we refer the interested reader to classical results on forcing schemes (*e.g.* [20]).

Let f^h be at least of class C^3 with respect to $\mathrm{D}/(\mathrm{D}t)$. We successively assume that $(\mathrm{D}/(\mathrm{D}t))^3 f_i^h \in \mathcal{O}(1)$ for $i = 0, 1, \ldots, q-1$ as functions of h. To derive the LBE, we use three discrete points in time $(t, t+h^2/2, t+h^2)$ (see Fig. 5), where the midpoint $t + h^2/2$ is a ghost node for the derivation and cancels in the final evolution equation of the scheme. Since the width of the stencil is mapped from the initial ϵ-scaling, limit consistency is ensured.

Definition 16. Let $g\colon \mathbb{R} \to \mathbb{R}, y \mapsto g(y)$ denote a C^∞-function and $a \in \mathbb{R}_{\geq 0}$ be a point on the non-negative real line. We define the following finite difference operations:

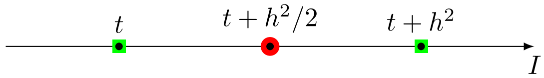

FIGURE 5. Time steps used for the space-time discretization. The final LBE operates on the green squares only. Red points are canceled in the derivation.

– Central difference

$$g'(y) = \frac{1}{a}\left(g\left(y+\frac{a}{2}\right) - g\left(y-\frac{a}{2}\right)\right) + \mathcal{O}\left(a^2\right), \tag{104}$$

– Forward difference

$$g'(y) = \frac{1}{a}\Big(g(y+a) - g(y)\Big) + \mathcal{O}(a), \tag{105}$$

– Taylor's theorem

$$g(y) = g(a) + g'(a)(y-a) + \mathcal{O}(|y-a|^2). \tag{106}$$

Starting with a central difference of $\mathrm{D}/(\mathrm{D}t)f_i^h$ at $t + h^2/2$ yields

$$h^2 \frac{\mathrm{D}}{\mathrm{D}t} f_i^h\left(t + \frac{1}{2}h^2\right) = f_i^h\left(t+h^2\right) - f_i^h(t) + R_{t,\boldsymbol{x}}^{(5)} \quad \text{in } I_h \times \Omega_h. \tag{107}$$

Taylor's theorem applied to f_i^h at at $t + h^2/2$ with the expansion point t, and a forward difference $(\mathrm{D}/(\mathrm{D}t))f_i^h$ at t yields

$$\begin{aligned} f_i^h\left(t+\frac{1}{2}h^2\right) &= f_i^h(t) + \frac{1}{2}h^2\frac{\mathrm{D}}{\mathrm{D}t}f_i^h(t) + R_{t,\boldsymbol{x}}^{(6)} \\ &= f_i^h(t) + \frac{1}{2}\left[f_i^h\left(t+h^2\right) - f_i^h(t)\right] + R_{t,\boldsymbol{x}}^{(7)} \end{aligned} \tag{108}$$

in $I_h \times \Omega_h$. Provided that $(\mathrm{D}/(\mathrm{D}t))^2 f_i^h \in \mathcal{O}(1)$ and $(\mathrm{D}/(\mathrm{D}t))^3 f_i^h \in \mathcal{O}(1)$, we deduce

– $R_{t,\boldsymbol{x}}^{(5)} \in \mathcal{O}(h^6)$,
– $R_{t,\boldsymbol{x}}^{(6)} \in \mathcal{O}(h^4)$, and
– $R_{t,\boldsymbol{x}}^{(7)} \in \mathcal{O}(h^4)$ for $(t,\boldsymbol{x}) \in I_h \times \Omega_h$.

To match the observation point for the discrete moments as functions of h, we shift $n_{\boldsymbol{f}^h}$ and $\boldsymbol{u}_{\boldsymbol{f}^h}$ by $h^2/2$, respectively in space-time. Recalling the diffusive limit (cf. (18) and (20)), $(\mathrm{D}/(\mathrm{D}t))n_{f^h} = 0$ and $(\mathrm{D}/(\mathrm{D}t))\boldsymbol{u}_{f^h} = 0$ instantly follows. Via $(\mathrm{D}/(\mathrm{D}t))$(82) and $(\mathrm{D}/(\mathrm{D}t))$(83), we have for $(t,x) \in I_h \times \Omega_h$ that

$$\frac{\mathrm{D}}{\mathrm{D}t} n_{\boldsymbol{f}^h} = \mathcal{O}(h^2), \tag{109}$$

$$\frac{\mathrm{D}}{\mathrm{D}t} \boldsymbol{u}_{\boldsymbol{f}^h} = \mathcal{O}(h). \tag{110}$$

Taylor expanding both (109) and (110) for $(t,x) \in I_h \times \Omega_h$ leads to the respective approximations

$$n_{\boldsymbol{f}^h}\left(t+\frac{1}{2}h^2\right) = n_{\boldsymbol{f}^h}(t) + \frac{1}{2}h^2\frac{\mathrm{D}}{\mathrm{D}t}n_{\boldsymbol{f}^h}(t) + R_{t,\boldsymbol{x}}^{(8)}$$

$$= n_{\boldsymbol{f}^h}(t) + R^{(9)}_{t,\boldsymbol{x}}, \tag{111}$$

$$\begin{aligned} \boldsymbol{u}_{\boldsymbol{f}^h}\left(t+\frac{1}{2}h^2\right) &= \boldsymbol{u}_{\boldsymbol{f}^h}(t) + \frac{1}{2}h^2 \frac{\mathrm{D}}{\mathrm{D}t}\boldsymbol{u}_{\boldsymbol{f}^h}(t) + R^{(10)}_{t,\boldsymbol{x}} \\ &= \boldsymbol{u}_{\boldsymbol{f}^h}(t) + R^{(11)}_{t,\boldsymbol{x}}. \end{aligned} \tag{112}$$

With remainder terms $R^{(8)}_{t,\boldsymbol{x}}, R^{(9)}_{t,\boldsymbol{x}}, R^{(10)}_{t,\boldsymbol{x}} \in \mathcal{O}(h^4)$ and $R^{(11)}_{t,\boldsymbol{x}} \in \mathcal{O}(h^3)$. At last, we compute the lattice Maxwellian for $(t,x) \in I_h \times \Omega_h$ with Taylor's theorem of (89) as

$$\overline{M}^{\mathrm{eq}}_{\boldsymbol{f}^h,i}\left(t+\frac{1}{2}h^2, x+v_i\frac{1}{2}h^2\right) = \overline{M}^{\mathrm{eq}}_{\boldsymbol{f}^h,i}(t,x) + R^{(12)}_{t,\boldsymbol{x}}. \tag{113}$$

To specify the error we use (111) and (112) for $\overline{M}^{\mathrm{eq}}_{\boldsymbol{f}^h,i}$ as given in (113). Further, from the meanwhile gathered assumptions that $(\mathrm{D}/(\mathrm{D}t))^j f_i^h \in \mathcal{O}(1)$ for $j = 0,1,2,3$ we deduce that $(\mathrm{D}/(\mathrm{D}t))\overline{M}^{\mathrm{eq}}_{\boldsymbol{f}^h,i} \in \mathcal{O}(1)$. Hence, being prefactored by h^2 in the leading order, the remainder $R^{(12)}_{t,\boldsymbol{x}} \in \mathcal{O}(h^2)$ for all $(t,\boldsymbol{x}) \in I_h \times \Omega_h$.

Definition 17. Based on the above discretizations (103), (107), (108), and (113), we construct the lattice Boltzmann equation (LBE) for a space-time cylinder $I_h \times \Omega_h$ and $i = 0,1,\ldots,q-1$ discrete velocities via reordering the terms of $(90)|_{(t+(1/2)h^2, x+\boldsymbol{v}_i(1/2)h^2)}$ to

$$f_i^h\left(t+h^2\right) - f_i^h(t) = -\frac{1}{3\nu+\frac{1}{2}}\left[f_i^h(t) - \overline{M}^{\mathrm{eq}}_{\boldsymbol{f}^h,i}(t)\right]. \tag{114}$$

Consequently, the family of LBEs reads

$$\mathcal{G} := \left(f_i^h\left(t+h^2\right) - f_i^h(t) + \frac{1}{3\nu+\frac{1}{2}}\left[f_i^h(t) - \overline{M}^{\mathrm{eq}}_{\boldsymbol{f}^h,i}(t)\right] = 0 \quad \text{in } I_h \times \Omega_h \times Q\right)_{h>0}. \tag{115}$$

3.4. Consistent lattice Boltzmann equations

Theorem 2. *Suppose that for given $h,\nu \in \mathbb{R}_{>0}$, f^h is a weak solution of the BGKBE (29) with moments n_{f^h} and $\boldsymbol{u}_{f^h}$. Further, let n_{f^h}, $\boldsymbol{u}_{f^h}$, $(\mathrm{D}/(\mathrm{D}t))^j f_i^h$ understood as functions of h fulfill that*

$$n_{f^h} \in \mathcal{O}(1) \quad \text{in } I_h \times \Omega_h, \tag{116}$$

$$\boldsymbol{u}_{f^h} \in \mathcal{O}(1) \quad \text{in } I_h \times \Omega_h, \tag{117}$$

$$\left(\frac{\mathrm{D}}{\mathrm{D}t}\right)^j f_i^h \in \mathcal{O}(1) \quad \text{in } I_h \times \Omega_h, \quad \text{for } j = 0,1,2,3, \tag{118}$$

for $i = 0,1,\ldots,q-1$. Then, the family $\mathcal{G}$ of LBEs is limit consistent of order two to the family $\mathcal{F}$ of BGKBEs in $I_h \times \Omega_h \times Q$.

Proof. Let f^h be a solution of the BGKBE (29) as specified above. Then Theorem 1 dictates the truncation error for discretizing Ξ down to Q. In particular, for all $i = 0,1,\ldots,q-1$

$$\mathcal{E}(h) \equiv \frac{6\nu}{6\nu+1}\left[h^2\frac{\mathrm{D}}{\mathrm{D}t}f_i^h + \frac{1}{3\nu}\left(f_i^h - \overline{M}^{\mathrm{eq}}_{\boldsymbol{f}^h,i}\right)\right] \in \mathcal{O}\left(h^2\right) \quad \text{in } I \times \Omega \times Q. \tag{119}$$

Considering $\mathcal{E}(h)|_{(t+(1/2)h^2, x+\boldsymbol{v}_i(1/2)h^2)}$ and substituting the Taylor expansions and finite differences constructed in (107), (108), and (113), unfolds that

$$\frac{6\nu}{6\nu+1}\left\{h^2\frac{\mathrm{D}}{\mathrm{D}t}f_i^h\left(t+\frac{1}{2}h^2\right) + \frac{1}{3\nu}\left[f_i^h\left(t+\frac{1}{2}h^2\right) - \overline{M}^{\mathrm{eq}}_{\boldsymbol{f}^h,i}\left(t+\frac{1}{2}h^2\right)\right]\right\}$$

$$\approx \frac{6\nu}{6\nu+1}\left(f_i^h\left(t+h^2\right)-f_i^h(t)+\frac{1}{3\nu}\left\{f_i^h(t)+\frac{1}{2}\left[f_i^h\left(t+h^2\right)-f_i^h(t)\right]-\overline{M}^{\mathrm{eq}}_{\boldsymbol{f}^h,i}(t)\right\}\right)$$
$$= f_i^h\left(t+h^2\right)-f_i^h(t)+\frac{1}{3\nu+\frac{1}{2}}\left[f_i^h(t)-\overline{M}^{\mathrm{eq}}_{\boldsymbol{f}^h,i}(t)\right]\in\mathcal{O}\left(h^2\right), \quad (120)$$

for $i=0,1,...,q-1$ and for all $t\in I_h$. The truncation error order is obtained by inserting the respective error terms $R^{(j)}_{t,\boldsymbol{x},\boldsymbol{v}}$ for $j=0,1,\ldots,12$. □

Proposition 3. *Assuming stability in terms of Definition 11, sufficiently smooth solutions to the family of LBEs $\mathcal{G}$ converge weakly to solutions of the incompressible NSE (1) with second-order limit-consistency and a truncation error $\mathcal{O}(\triangle x^2)$.*

Proof. Since we have merged two limit-consistent discretizations (velocity and space-time) to obtain the discrete family $\mathcal{G}$ the abstract setting for Lemma 2 is similarly verified as in the proof of Proposition 2. The weak convergence of $\mathcal{G}$ with second order consistent discretization with $\epsilon \leftarrow\!\!\!\shortmid h = \triangle x \sim \sqrt{\triangle t}$ is then determined via the concatenation of weak solution functors

$$\mathcal{G}\xrightarrow[\mathcal{O}(h^2)]{h\searrow 0}\mathrm{NSE}\equiv\left(\mathcal{F}\xrightarrow[\mathcal{O}(\epsilon^2)]{\epsilon\searrow 0}\mathrm{NSE}\right)\circ\left(\mathcal{G}\xrightarrow[\mathcal{O}(h^2)]{h\searrow 0}\mathcal{F}\right) \quad (121)$$

according to Lemma 2. □

Remark 17. Here, we effectively derive the LBE by chaining Taylor expansions and finite differences with the inclusion of a shift by half the space-time grid spacing. As suggested in the literature [15,59], the latter substitutes the implicity, resembles a Crank–Nicolson scheme, and unfolds the LBE as a finite difference discretization of the BGKBE. In addition, we couple the discretization to a sequencing parameter, which is responsible for the weak convergence of mesoscopic solutions to solutions of the macroscopic target PDE. This finding aligns with recent work [6,7] that rigorously expresses LBMs in terms of finite differences of macroscopic variables.

Remark 18. Although we assumed an isothermal configuration in the present manuscript, an extension to the non-uniform temperature case should be realizable. Since the continuous thermal limit is rigorously proven in [48], a suitable discretization, *e.g.* including an equilibrium function approximation of higher orders and larger velocity stencils, should be limit consistent as well.

4. Conclusion

The notion of limit consistency is introduced for the constructive discretization towards an LBM for a given PDE. In particular, a family of LBEs $\mathcal{G}$ is consistently derived from a family of BGKBEs $\mathcal{F}$ which is known to rigorously limit towards a given partial differential IVP in the sense of weak solutions. Preparatively, the discrete velocity BGKBE $\mathcal{FG}$ is constructed by replacing the velocity space with a discrete subset. When completed, we discretize continuous space and time by chaining several finite-difference approximations, which leads to $\mathcal{G}$. In the present example, all of the discrete operations retain the diffusive limit of the BGKBE towards the NSE on the continuous level.

It should be noted that the term consistency in the derivation process refers to the level-by-level preservation of the *a priori* proven limit in a formal, weak or strong sense, respectively. As such, our approach presents itself as a mathematically tractable discretization procedure, which produces a numerical scheme with a proven limit towards the target equation under diffusive scaling. Although the incompressible NSE are used as an example target system, the current approach is extendable to any other PDE. In addition, the notion of limit consistency is flexible in the sense that it can be applied to relaxation systems without the knowledge of an underlying kinetic equation system limiting to the targeted PDE. Hence, the sole constraint remaining is the existence of an *a priori* known continuous moment limit which dictates the relaxation process.

It is important to further isolate the differences and advantages of our approach with respect to classical consistency and asymptotic preservation analysis. The mapping of parameters $\epsilon \leftarrow\!\shortmid h$ is restrictive exactly in the sense that it is irreversible. However, the mapping itself is not a necessary step in general. If the aim is to evaluate the consistency of the numerical scheme for the complete spaces of the individual parameters, it would indeed be a wise decision to not map the parameters and continue with multiple ones. Nonetheless, as LBMs often do target macroscopic (relaxed) PDEs, the mapping of parameters is required to reach this limit when refining the space-time discretization. Specifically, for the application case considered here (incompressible NSE), a limit with constant Mach or Knudsen number is not of interest. The macroscopic PDE can therefore only be reached when both ϵ and h are decreased in a specific ratio (diffusive scaling), which renders all other cases irrelevant in this setting.

Further, we provide a successive discretization by nesting conventional Taylor expansions and finite differences. The estimation of the truncation errors at all levels within the derivation enables us to track the discretization state of the equations. Parametrizing the latter in advance allows us to predetermine the link of discrete and relaxation parameters, which is primarily relevant to uphold the path towards the targeted PDE. The unfolding of the LBM as a chain of finite differences and Taylor expansions under the relaxation constraint matches the results in the literature [7, 25] and thus validates the present work. Although similarities with well-established references [26, 28] are present, it should be stressed that the purpose of limit consistency is to touch base with the previous construction steps [53, 56]. By assembling the perturbative construction of generic relaxation systems proposed in [53, 56] with the consistent discretization here derived, we enable a generic top-down design of LBMs. Future studies as prepared in [49] will complete the coherent top-down procedure to derive LBMs for large classes of PDEs.

Funding

The authors thank the anonymous reviewers for their helpful comments. This work was partially funded by the "Deutsche Forschungsgemeinschaft" (DFG, German Research Foundation) – project 382064892, KR 4259/8-2.

Data availability statement

The research data associated with this article are included in the article.

Author contribution statement

S. Simonis: Conceptualization, Methodology, Formal analysis, Validation, Investigation, Visualization, Writing – Original draft, Writing – Review & Editing, Project administration, Resources; M. J. Krause: Conceptualization, Writing – Review & Editing, Supervision, Funding acquisition. All authors read and approved the final manuscript.

References

[1] H. Babovsky, *Die Boltzmann-Gleichung: Modellbildung-Numerik-Anwendungen*. Springer Vieweg + Teubner (1998). https://doi.org/10.1007/978-3-663-12034-6.

[2] P. Bachmann, *Die analytische Zahlentheorie*. Teubner (1923).

[3] M. Banda, A. Klar, L. Pareschi, and M. Seaid, Lattice-Boltzmann type relaxation systems and high order relaxation schemes for the incompressible Navier-Stokes equations. *Math. Comput.* **77** (2008) 943–965. https://doi.org/10.1090/S0025-5718-07-02034-0.

[4] C. Bardos, F. Golse, and C.D. Levermore, Fluid dynamic limits of kinetic equations II: Convergence proofs for the Boltzmann equation. *Commun. Pure Appl. Math.* **46** (1993) 667–753. https://doi.org/10.1002/cpa.3160460503.

[5] S. Bartels, *Numerical methods for nonlinear partial differential equations*, vol. **47**. Springer Cham (2015). https://doi.org/10.1007/978-3-319-13797-1.

[6] T. Bellotti, Truncation errors and modified equations for the lattice Boltzmann method via the corresponding finite difference schemes. *ESAIM Math. Model. Num. Anal.* **57** (2023) 1225–1255. https://doi.org/10.1051/m2an/2023008.

[7] T. Bellotti, B. Graille, and M. Massot, Finite difference formulation of any lattice Boltzmann scheme. *Numer. Math.* **152** (2022) 1–40. https://doi.org/10.1007/s00211-022-01302-2.

[8] P. L. Bhatnagar, E.P. Gross, and M. Krook, A model for collision processes in gases. I. Small amplitude processes in charged and neutral one-component systems. *Phys. Rev. E* **94** (1954) 511–525. https://doi.org/10.1103/PhysRev.94.511.

[9] B.M. Boghosian, J. Yepez, P.V. Coveney, and A. Wagner, Entropic lattice Boltzmann methods. *Proc. R. Soc. A* **457** (2007) 717–766. https://doi.org/10.1098/rspa.2000.0689.

[10] F. Bouchut, F.R. Guarguaglini, and R. Natalini, Diffusive BGK approximations for nonlinear multidimensional parabolic equations. *Indiana Univ. Math. J.* **49** (2000) 723–749. https://doi.org/10.1512/iumj.2000.49.1811.

[11] F. Caetano, F. Dubois, and B. Graille, A result of convergence for a mono-dimensional two-velocities lattice Boltzmann scheme. *Discrete Contin. Dyn. Syst. – S* **17** (2024) 3129–3154. https://doi.org/10.3934/dcdss.2023072.

[12] A. Caiazzo, M. Junk, and M. Rheinländer, Comparison of analysis techniques for the lattice Boltzmann method. *Comput. Math. Appl.*, **58** (2009) 883–897. https://doi.org/10.1016/j.camwa.2009.02.011.

[13] T.H. Cormen, C.E. Leiserson, R.L. Rivest, and C. Stein, *Introduction to Algorithms*. The MIT Press (2022).

[14] D. Dapelo, S. Simonis, M.J. Krause, and J. Bridgeman, Lattice-Boltzmann coupled models for advection-diffusion flow on a wide range of Péclet numbers. *J. Comput. Sci.* **51** (2021) 101363. https://doi.org/10.1016/j.jocs.2021.101363.

[15] P.J. Dellar, An interpretation and derivation of the lattice Boltzmann method using Strang splitting. *Comput. Math. Appl.* **65** (2013) 129–141. https://doi.org/10.1016/j.camwa.2011.08.047.

[16] F. Dubois, Equivalent partial differential equations of a lattice Boltzmann scheme. *Comput. Math. Appl.* **55** (2008) 1441–1449. https://doi.org/10.1016/j.camwa.2007.08.003.

[17] B.H. Elton, C.D. Levermore, and G.H. Rodrigue, Convergence of Convective-Diffusive Lattice Boltzmann Methods. *SIAM J. Numer. Anal.* **32** (1995) 1327–1354. https://doi.org/10.1137/0732062.

[18] G.B. Folland, *Advanced Calculus*. Pearson Education (US) (2001).

[19] A.N. Gorban, Hilbert's sixth problem: the endless road to rigour. *Philos. Trans. A Math. Phys. Eng. Sci.* **376** (2018) 20170238. https://doi.org/10.1098/rsta.2017.0238.

[20] Z. Guo, C. Zheng, and B. Shi, Discrete lattice effects on the forcing term in the lattice Boltzmann method. *Phys. Rev. E* **65** (2002) 046308. https://doi.org/10.1103/PhysRevE.65.046308.

[21] Z. Guo, J. Li, and K. Xu, Unified preserving properties of kinetic schemes. *Phys. Rev. E* **107** (2023) 025301. https://doi.org/10.1103/PhysRevE.107.025301.

[22] M. Haussmann, P. Reinshaus, S. Simonis, H. Nirschl, and M.J. Krause, Fluid-structure interaction simulation of a coriolis mass flowmeter using a lattice Boltzmann method. *Fluids* **6** (2021) 167. https://doi.org/10.3390/fluids6040167.

[23] X. He and L.-S. Luo, Theory of the lattice Boltzmann method: from the Boltzmann equation to the lattice Boltzmann equation. *Phys. Rev. E* **56** (1997) 6811–6817. https://doi.org/10.1103/PhysRevE.56.6811.

[24] S. Jin, Asymptotic preserving (AP) schemes for multiscale kinetic and hyperbolic equations: a review. *Riv. Mat. Univ. Parma.* **3** (2012) 177–216. https://ins.sjtu.edu.cn/people/shijin/PS/AP.pdf.

[25] M. Junk, A finite difference interpretation of the lattice Boltzmann method. *Numer. Methods Partial Differ. Equ.* **17** (2001) 383–402. https://doi.org/10.1002/num.1018.

[26] M. Junk and A. Klar, Discretizations for the incompressible Navier-Stokes equations based on the Lattice Boltzmann method. *SIAM J. Sci. Comput.* **22** (2000) 1–19. https://doi.org/10.1137/S1064827599357188.

[27] M. Junk and W.-A. Yong, Weighted $\mathbb{L}^2$-stability of the Lattice Boltzmann method. *SIAM J. Numer. Anal.* **47** (2009) 1651–1665. https://doi.org/10.1137/060675216.

[28] M. Junk, A. Klar, and L.-S. Luo, Asymptotic analysis of the lattice Boltzmann equation. *J. Comput. Phys.* **210** (2005) 676–704. https://doi.org/10.1016/j.jcp.2005.05.003.

[29] I.V. Karlin, A. Ferrante, and H.C. Öttinger, Perfect entropy functions of the Lattice Boltzmann method. *Europhys. Lett.* **47** (1999) 182–188. https://doi.org/10.1209/epl/i1999-00370-1.

[30] A. Klar, Relaxation scheme for a Lattice–Boltzmann-type discrete velocity model and numerical Navier–Stokes limit. *J. Comput. Phys.* **148** (1999) 416–432. https://doi.org/10.1006/jcph.1998.6123.

[31] M.J. Krause, Fluid flow simulation and optimisation with Lattice Boltzmann methods on high performance computers – application to the human respiratory system. *Doctoral thesis*, Karlsruhe Institute of Technology (KIT) (2010). https://doi.org/10.5445/IR/1000019768; https://publikationen.bibliothek.kit.edu/1000019768.

[32] M.J. Krause, A. Kummerländer, S.J. Avis, H. Kusumaatmaja, D. Dapelo, F. Klemens, M. Gaedtke, N. Hafen, A. Mink, R. Trunk, J.E. Marquardt, M.-L. Maier, M. Haussmann, and S. Simonis, OpenLB – Open source lattice Boltzmann code. *Comput. Math. Appl.* **81** (2021) 258–288, 2021. https://doi.org/10.1016/j.camwa.2020.04.033.

[33] E. Kummer and S. Simonis, Nonuniqueness of lattice Boltzmann schemes derived from finite difference methods. *Ex. Counterex.* **7** (2025) 100171. https://doi.org/10.1016/j.exco.2024.100171.

[34] A. Kummerländer, S. Avis, H. Kusumaatmaja, F. Bukreev, D. Dapelo, S. Großmann, N. Hafen, C. Holeksa, A. Husfeldt, J. Jeßberger, L. Kronberg, J. Marquardt, J. Mödl, J. Nguyen, T. Pertzel, S. Simonis, L. Springmann, N. Suntoyo, D. Teutscher, M. Zhong, and M. Krause, *OpenLB Release 1.5: Open source lattice Boltzmann code*, November (2022).https://doi.org/10.5281/zenodo.6469606.

[35] P. Lallemand and L.-S. Luo, Theory of the lattice Boltzmann method: Dispersion, dissipation, isotropy, Galilean invariance, and stability. *Phys. Rev. E* **61** (2000) 6546–6562. https://doi.org/10.1103/PhysRevE.61.6546.

[36] P. Lallemand, L.-S. Luo, M. Krafczyk, and W.-A. Yong, The lattice Boltzmann method for nearly incompressible flows. *J. Comput. Phys.* **431** (2021) 109713. https://doi.org/10.1016/j.jcp.2020.109713.

[37] E. Landau, *Handbuch der Lehre von der Verteilung der Primazahlen.* BG Teubner (1909).

[38] P.D. Lax and R.D. Richtmyer, Survey of the stability of linear finite difference equations. *Commun. Pure Appl. Math.* **9** (1956) 267–293. https://doi.org/10.1002/cpa.3160090206.

[39] J. Leray, Sur le mouvement d'un liquide visqueux emplissant l'espace. *Acta Math.* **63** (1934) 193–248. https://doi.org/10.1007/BF02547354.

[40] R.J. LeVeque, *Finite difference methods for ordinary and partial differential equations: steady-state and time-dependent problems.* SIAM (2007). https://doi.org/10.1137/1.9780898717839.

[41] P.-A. Masset and G. Wissocq, Linear hydrodynamics and stability of the discrete velocity Boltzmann equations. *J. Fluid Mech.* **897** (2020) A29. https://doi.org/10.1017/jfm.2020.374.

[42] A. Mink, K. Schediwy, C. Posten, H. Nirschl, S. Simonis, and M.J. Krause, Comprehensive computational model for coupled fluid flow, mass transfer, and light supply in tubular photobioreactors equipped with glass sponges. *Energies* **15** (2022) 7671. https://doi.org/10.3390/en15207671.

[43] S. Mischler, Uniqueness for the BGK-equation in $\mathbb{R}^N$ and rate of convergence for a semi-discrete scheme. *Diff. Integral Equ.* **9** (1996) 1119–1138. https://doi.org/10.57262/die/1367871533.

[44] J.A. Murdock, *Perturbations: Theory and Methods.* SIAM (1999).

[45] B. Perthame, Global existence to the BGK model of Boltzmann equation. *J. Diff. Equ.* **82** (1989) 191–205. https://doi.org/10.1016/0022-0396(89)90173-3.

[46] B. Perthame and M. Pulvirenti, Weighted L^∞ bounds and uniqueness for the Boltzmann BGK model. *Arch. Ration. Mechan. Anal.* **125** (1993) 289–295. https://doi.org/10.1007/BF00383223.

[47] L. Saint-Raymond, Discrete time Navier-Stokes limit for the BGK Boltzmann equation. *Commun. Partial Differ. Equ.* **27** (2002) 149–184. https://doi.org/10.1081/PDE-120002785.

[48] L. Saint-Raymond, From the BGK model to the Navier-Stokes equations. *Ann. Sci. Ec. Norm. Super.* **36** (2023) 271–317. https://doi.org/10.1016/S0012-9593(03)00010-7.

[49] S. Simonis, *Lattice Boltzmann methods for partial differential equations.* Doctoral thesis, Karlsruhe Institute of Technology (KIT) (2023). https://doi.org/10.5445/IR/1000161726; https://publikationen.bibliothek.kit.edu/1000161726.

[50] S. Simonis, N. Hafen, J. Jeßberger, D. Dapelo, G. Thäter, M. J. Krause, Homogenized lattice Boltzmann methods for fluid flow through porous media – Part I: Kinetic model derivation. *ESAIM: M2AN* **59** (2025) 789–813, 2025. https://doi.org/10.1051/m2an/2025005.

[51] S. Simonis and M. J. Krause, Forschungsnahe Lehre unter Pandemiebedingungen. *Mitt. Deutsche Math. Ver.* **30** (2022) 43–45. https://doi.org/10.1515/dmvm-2022-0015.

[52] S. Simonis and S. Mishra, Computing statistical Navier–Stokes solutions, in *Hyperbolic balance laws: interplay between scales and randomness (Oberwolfach Report 21)*, Edited by R. Abgrall, M. Garavello, M. Lukáčová-Medvid'ová, and K. Trivisa (2024) 634–637. https://doi.org/10.4171/OWR/2024/10.

[53] S. Simonis, M. Frank, and M.J. Krause, On relaxation systems and their relation to discrete velocity Boltzmann models for scalar advection–diffusion equations. *Philos. Trans. R. Soc. London. Ser. A* **378** (2020) 20190400. https://doi.org/10.1098/rsta.2019.0400.

[54] S. Simonis, M. Haussmann, L. Kronberg, W. Dörfler, and M.J. Krause, Linear and brute force stability of orthogonal moment multiple-relaxation-time lattice Boltzmann methods applied to homogeneous isotropic turbulence. *Philos. Trans. R. Soc. London. Ser. A* **379** (2021) 20200405. https://doi.org/10.1098/rsta.2020.0405.

[55] S. Simonis, D. Oberle, M. Gaedtke, P. Jenny, and M. J. Krause, Temporal large eddy simulation with lattice Boltzmann methods. *J. Comput. Phys.* **454** (2022) 110991. https://doi.org/10.1016/j.jcp.2022.110991.

[56] S. Simonis, M. Frank, and M. J. Krause, Constructing relaxation systems for lattice Boltzmann methods. *Appl. Math. Lett.* **137** (2023) 108484. https://doi.org/10.1016/j.aml.2022.108484.

[57] M. Siodlaczek, M. Gaedtke, S. Simonis, M. Schweiker, N. Homma, and M.J. Krause, Numerical evaluation of thermal comfort using a large eddy lattice Boltzmann method. *Build. Environ.* **192** (2021) 107618. https://doi.org/10.1016/j.buildenv.2021.107618.

[58] E. Tadmor, A review of numerical methods for nonlinear partial differential equations. *Bull. Amer. Math. Soc.* **49** (2012) 507–554. https://doi.org/10.1090/S0273-0979-2012-01379-4.

[59] S. Ubertini, P. Asinari, and S. Succi, Three ways to lattice Boltzmann: A unified time-marching picture. *Phys. Rev. E*, **81** (2010) 016311. https://doi.org/10.1103/PhysRevE.81.016311.

[60] G. Wissocq and P. Sagaut, Hydrodynamic limits and numerical errors of isothermal lattice Boltzmann schemes. *J. Comput. Phys.* **450** (2022) 110858. https://doi.org/10.1016/j.jcp.2021.110858.

[61] D. A. Wolf-Gladrow, *Lattice-Gas Cellular Automata and Lattice Boltzmann Models: An Introduction. Lecture Notes in Mathematics.* Springer Berlin, Heidelberg (2000). https://doi.org/10.1007/b72010.

[62] W. Zhao and W.-A. Yong, Maxwell iteration for the lattice Boltzmann method with diffusive scaling. *Phys. Rev. E* **95** (2017) 033311. https://doi.org/10.1103/PhysRevE.95.033311.

Appendix A. Notation

This section summarizes the notation used in this paper, both classical and unconventional ones.

A.1. Bachmann–Landau notation

Since smallness parameters such as ϵ and h are essential in the present context, we use the Bachmann–Landau notation [2,37] for asymptotically bounding functions of *e.g.* ϵ when $\epsilon \searrow 0$.

Definition 18. Let $g(\epsilon)$ be a given monotone function on a subset of $\mathbb{R}_{>0}$, which is asymptotically positive (*i.e.* $g(\epsilon) > 0$ for sufficiently small $\epsilon < \epsilon_1$). Then, $\mathcal{O}(g(\epsilon))$ denotes the set of functions

$$\mathcal{O}(g(\epsilon)) = \left\{ f(\epsilon) \,\middle|\, \exists c, \epsilon_1 > \epsilon_0 > 0 \colon \left| f(\epsilon) \right| \leq c g(\epsilon) \ \forall 0 < \epsilon < \epsilon_0 \right\}. \tag{A.1}$$

Remark 19. Despite $\mathcal{O}(g(\epsilon))$ being a set [13], below we occasionally align with common practice by writing for an exemplary real- or complex-valued function $f(\epsilon)$ that $f(\epsilon) = \mathcal{O}(g(\epsilon))$ instead of $f(\epsilon) \in \mathcal{O}(g(\epsilon))$. The equality sign is motivated by the observation that if $f(\epsilon) = \mathcal{O}(g(\epsilon))$, then $f(\epsilon)$ is equal to $g(\epsilon)$ within a constant factor such that $g(\epsilon)$ is an asymptotic bound for $f(\epsilon)$. Also in this regard, unless stated otherwise, we assume that the function space affiliation of $g(\epsilon)$ carries over to $\mathcal{O}(g(\epsilon))$. In the case where we are dealing with tensors, the notation $\mathcal{O}(\cdot)$ should be understood for each element. Finally, it should be stressed that in the present context, the $\mathcal{O}$-notation is not understood in a formal sense only, where the terms of a series are substituted. Instead, we make use of the $\mathcal{O}$-notation to actually refer to estimates of errors in approximate solutions [44] whenever the rigor is possible and use the formal sense as a fallback.

A.2. Notions of convergence

We frequently use the following classical notions of convergence which are recalled here for the sake of clarity.

Definition 19. Let X^* be the dual space of a normed space (*e.g.* a Hilbert space) X. In general, (x_n) in X converges weakly to $x \in X$ if the sequence of scalars $(f(x_n))$ converges to $f(x)$ $\forall f \in X^*$.

Lemma 4. *If (x_n) is (strongly) convergent to x in X, then (x_n) is weakly convergent to x.*

Definition 20. A sequence $(f_n) \subseteq X^*$ is weak-* convergent to $f \in X^*$ if $(f_n(x))$ converges to $f(x)$ $\forall x \in X$.

Lemma 5. *If $(f_n) \subseteq X^*$ converges weakly to $f \in X^*$, then (f_n) is weak-* convergent to f.*

Definition 21. Let the dual of L^p be denoted as $L^{p'}$, where $p' = p/(p-1)$ is the conjugate exponent. In case of $p = 1$, $p' = \infty$. For $1 \geq p \geq \infty$ we define

$$w - L^p := \begin{cases} \text{weak topology } \sigma\left(L^p, L^{p'}\right) & \text{if } p < \infty, \\ \text{weak-}^* \text{ topology } \sigma\left(L^\infty, L^1\right) & \text{if } p = \infty. \end{cases} \tag{A.2}$$

To connect these classical notions of weak convergence to the here used Bachmann–Landau notation, we make use of the following lemma.

Lemma 6. *Let H be a Hilbert space with inner product $\langle \cdot, \cdot \rangle_H$. Furthermore, let $u^\epsilon, u_0 \in H$ and assume that u^ϵ converges weakly to u_0, i.e. for every $\phi \in H$, that is*

$$\left\langle u^\epsilon - u_0, \phi \right\rangle_H \to 0, \quad \textit{for } \epsilon \to 0. \tag{A.3}$$

Assume further that u^ϵ admits the asymptotic expansion

$$u^\epsilon = u_0 + \epsilon g_1 + O(\epsilon^2), \tag{A.4}$$

for some $g_1 \in H$. Then, we obtain the Bachmann–Landau order estimate

$$\left\langle u^\epsilon - u_0, \phi \right\rangle_H = \mathcal{O}(\epsilon). \tag{A.5}$$

Proof. Since u^ϵ is assumed to have an asymptotic expansion, we can test it against some function ϕ using the linearity of the inner product

$$\mathfrak{I}^\epsilon = \left\langle u^\epsilon - u_0, \phi \right\rangle_H = \epsilon \left\langle g_1, \phi \right\rangle_H + \mathcal{O}(\epsilon^2). \tag{A.6}$$

When taking the lower limit, we obtain

$$\liminf_{\epsilon \to 0} \frac{|I^\epsilon|}{\epsilon} \leq C \left\|\phi\right\|_H \left\|g_1\right\|_H, \tag{A.7}$$

for a constant C. Since weak convergence implies that the leading-order term vanishes for $\epsilon \to 0$, we conclude

$$\mathfrak{I}^\epsilon = \mathcal{O}\big(\epsilon\big). \tag{A.8}$$

□

In addition, we point out that given sufficient smoothness of a weakly convergent function in the expansion parameter, we can deduce the order of convergence by the following lemma.

Lemma 7. *Let H be a Hilbert space with inner product $\langle \cdot, \cdot \rangle_H$. Furthermore, let $u^\epsilon, u_0 \in H$ and assume that u^ϵ converges weakly to u_0 in H. If the function u_0 is r-times differentiable with respect to ϵ, i.e. there exist derivatives u_k such that*

$$\frac{\partial^k u}{\partial \epsilon^k} = u_k, \quad \textit{for } k = 1, \ldots, r, \tag{A.9}$$

then

$$u^\epsilon = u_0 + \mathcal{O}(\epsilon^r). \tag{A.10}$$

Proof. Since u^ϵ is assumed to be r-times differentiable in ϵ, we can expand it in a Taylor series around $\epsilon = 0$, *i.e.*

$$u^\epsilon = u_0 + \epsilon u_1 + \frac{\epsilon^2}{2!}u_2 + \cdots + \frac{\epsilon^r}{r!}u_r + \mathcal{O}(\epsilon^{r+1}). \tag{A.11}$$

We show that weak convergence ensures that the first $r-1$ terms vanish asymptotically. Applying the weak convergence condition, where $\phi \in H$ is any test function, we have

$$\left\langle u^\epsilon - u_0, \phi\right\rangle_H \to 0, \quad \text{for } \epsilon \to 0. \tag{A.12}$$

Based on the Taylor expansion, we obtain

$$\left\langle \epsilon u_1 + \frac{\epsilon^2}{2!}u_2 + \cdots + \frac{\epsilon^r}{r!}u_r + \mathcal{O}(\epsilon^{r+1}), \phi\right\rangle_H \to 0. \tag{A.13}$$

Since this holds for all test functions ϕ, we conclude that the weak limit of each term vanishes, ensuring that their contributions to the norm decay at least as fast as $\mathcal{O}(\epsilon^r)$. Norming both sides of the expansion yields

$$\|u^\epsilon - u_0\|_H = \mathcal{O}(\epsilon^r), \tag{A.14}$$

which implies the desired result. □

Appendix B. Continuous diffusive limit

We recall the main result of Saint-Raymond [48] in the present notation. It is to be stressed that the present work neglects the additional temperature equation appearing in the limit via imposing an ideal gas. Let the Hilbert space $L^2(\mathbb{R}^d, M\,\mathrm{d}\boldsymbol{v})$ be defined by the scalar product

$$(f, g) \mapsto \int_{\mathbb{R}^d} f(\boldsymbol{v}) g(\boldsymbol{v}) M(\boldsymbol{v})\,\mathrm{d}\boldsymbol{v}, \tag{B.15}$$

where $M\,\mathrm{d}\boldsymbol{v}$ is a positive unit measure on $\mathbb{R}^d$ which allows the definition of an average

$$\left\langle \xi \right\rangle := \int_{\mathbb{R}^d} \xi(\boldsymbol{v})\, M(\boldsymbol{v})\,\mathrm{d}\boldsymbol{v} \tag{B.16}$$

over $\Xi = \mathbb{R}$ for any integrable function ξ.

Definition 22. For any pair (f, g) of functions which are measurable and almost everywhere non-negative on $\mathfrak{P}$, define the relative entropy

$$H(f \mid g) := \int_{\mathbb{R}^d}\int_{\mathbb{R}^d} \left(f \log\left(\frac{f}{g}\right) - f + g\right) \mathrm{d}\boldsymbol{v}\,\mathrm{d}\boldsymbol{x} \geq 0. \tag{B.17}$$

Based on that, we recall the following preparative result from [47]. Note that locally integrable functions on $X \subseteq \mathbb{R}^d$ and Sobolev spaces based on L^2 are denoted with

$$L^1_{\mathrm{loc}}(X) = \left\{ f\colon X \to \mathbb{R} \;\middle|\; \forall \boldsymbol{x} \in X\, \exists r > 0\colon\; B_r(\boldsymbol{x}) \subseteq X \,\wedge\, f|_{B_r(\boldsymbol{x})} \in L^1(B_r(\boldsymbol{x})) \right\}, \tag{B.18}$$

$$H^k(X) = W^{k,2}(X) = \left\{ f \in L^2(X) \;\middle|\; \forall |\alpha| \leq k\, \exists \text{ weak derivative } \partial^\alpha f \in L^2(X) \right\}, \tag{B.19}$$

respectively. The latter are Hilbert spaces and the dual of $H^k(X)$ is denoted with $H^{-k}(X)$.

Theorem 3. *Let $\epsilon > 0$ and $0 \leq f^0_\epsilon \in L^1_{\mathrm{loc}}(\mathfrak{P})$ such that the entropy is bounded $H(f^0_\epsilon \mid M) < \infty$. Then $\exists\, f_\epsilon$ a global, non-negative, and weak solution of (29) which fulfills*

$$f_\epsilon - M \in C\left(\mathbb{R}_{>0}, L^2(\mathfrak{P}) + L^1(\mathfrak{P})\right) \tag{B.20}$$

and $\forall t > 0$*:*

$$H\left(f_\epsilon(t) \mid M\right) + \frac{1}{\epsilon^2 \nu} \int_0^t \int_{\mathbb{R}^d} \int_{\mathbb{R}^d} D\left(f_\epsilon\right)(s) \, \mathrm{d}\boldsymbol{v} \, \mathrm{d}\boldsymbol{x} \, \mathrm{d}s \leq H\left(f_\epsilon^0 \mid M\right), \tag{B.21}$$

where the dissipation $D(f_\epsilon)$ *is defined by*

$$D\left(f_\epsilon\right) = \left(M_{f_\epsilon} - f_\epsilon\right) \log\left(\frac{M f_\epsilon}{f_\epsilon}\right) \geq 0. \tag{B.22}$$

Additionally, the weak solution fulfills the typical moment integrated conservation laws (13)*,* (14)*, and* (15) *at zeroth, first, and second order, respectively.*

Proof. This theorem has been stated and proven in [47]. □

Via a boundedness assumption in $L^2(\mathfrak{P}, \mathrm{d}\boldsymbol{x} M \, \mathrm{d}\boldsymbol{v})$ of initial sequential fluctuation data (g_ϵ^0) defined from

$$g_\epsilon^0 = \frac{1}{\epsilon}\left(\frac{f_\epsilon^0}{M} - 1\right), \tag{B.23}$$

a constantly prefactored entropy bound $C_0 \epsilon^2$ is obtained, and in turn, weak compactness on $(M g_\epsilon)$ holds in $L^1_{\mathrm{loc}}(\mathbb{R}_{>0} \times \mathbb{R}^d, L^1(\mathbb{R}^d))$ [4, 48]. We can thus transfer the main result of [48] to the isothermal setting.

Theorem 4. *Let* (g_ϵ^0) *be a family of measurable functions on* $\mathfrak{P}$ *which satisfy*

$$1 + \epsilon g_\epsilon^0 \geq 0 \text{ almost everywhere}, \tag{B.24}$$

$$H\left(M\left(1 + \epsilon g_\epsilon^0\right) \mid M\right) \leq C_0 \epsilon^2, \tag{B.25}$$

and with $\boldsymbol{\nabla}_{\boldsymbol{x}} \cdot \boldsymbol{u}_0 = 0$ *additionally fulfill that*

$$\left\langle g_\epsilon^0 \boldsymbol{v} \right\rangle \xrightarrow[w-L^2\left(\mathbb{R}^d\right)]{\epsilon \searrow 0} \boldsymbol{u}_0 \tag{B.26}$$

Further, let $f_\epsilon = M(1 + \epsilon g_\epsilon)$ *be a solution of* (29)*. Then*

$$\exists \rho, \boldsymbol{u} \in L^\infty\left(\mathbb{R}_{>0}, L^2\left(\mathbb{R}^d\right)\right) \cap L^2\left(\mathbb{R}_{>0}, H^1\left(\mathbb{R}^d\right)\right) \tag{B.27}$$

we have weak convergence such that, modulo a zero-limiting subsequence (ϵ_n)*,*

$$\left\langle g_\epsilon \right\rangle \xrightarrow[w-L^1_{\mathrm{loc}}\left(\mathbb{R}_{>0} \times \mathbb{R}^d\right)]{\epsilon \searrow 0} \rho, \tag{B.28}$$

$$\left\langle g_\epsilon \boldsymbol{v} \right\rangle \xrightarrow[w-L^1_{\mathrm{loc}}\left(\mathbb{R}_{>0} \times \mathbb{R}^d\right)]{\epsilon \searrow 0} \boldsymbol{u}. \tag{B.29}$$

In addition, ρ *and* $\boldsymbol{u}$ *are weak solutions of the incompressible NSE* (1)*, where the pressure is determined from the solenoidal condition.*

Proof. An extended version of this theorem (considering non-uniform temperature) has been stated and proven in [48]. □